8.07f/W(Jul162004) +model | MPS : 1498 | Prod.Type:FTP pp.1–38(col.fig.:NIL) | ED:AnupamaDeviY PAGN:Bas SCAN:

ARTICLE IN PRESS

Available online at www.sciencedirect.com
ScienceDirect
Journal of the Mechanics and Physics of Solids
▮ (▮▮▮▮) ▮▮▮–▮▮▮

JOURNAL OF THE MECHANICS AND PHYSICS OF SOLIDS

www.elsevier.com/locate/jmps

Bi-functional optimization of actively cooled, pressurized hollow sandwich cylinders with prismatic cores

T. Liu[a], Z.C. Deng[a,b,*], T.J. Lu[c]

[a]*Department of Engineering Mechanics, Northwestern Polytechnical University, Xi'an 710072, PR China*
[b]*State Key Laboratory of Structural Analysis of Industrial Equipment, Dalian University of Technology, Dalian 116024, PR China*
[c]*MOE Key Laboratory of Strength and Vibration, School of Aerospace, Xi'an Jiaotong University, Xi'an 710049, PR China*

Received 7 December 2006; received in revised form 14 April 2007; accepted 22 April 2007

Abstract

All metallic, hollow sandwich cylinders having ultralight two-dimensional (2D) prismatic cores are optimally designed for maximum thermo-mechanical performance at minimum mass. The heated cylinder is subjected to uniform internal pressure and actively cooled by forced air convection. The use of two different core topologies is exploited: square- and triangular-celled cores. The minimum mass design model is so defined that three failure modes are prevented: facesheet yielding, core member yielding, and core member buckling. The intersection-of-asymptotes method, in conjunction with the fin analogy model, is employed to build the optimization model for maximum heat transfer rate. A non-dimensional parameter is introduced to couple the two objectives—structural and thermal—in a single cost function. It is found that the geometry corresponding to maximum heat transfer rate is not unique, and square-celled core sandwich cylinders outperform those having triangular cells. The eight-layered sandwich cylinders with square cells have the best overall performance in comparison with other core topologies. Whilst a sandwich cylinder with shorter

*Corresponding author. Department of Engineering Mechanics, Northwestern Polytechnical University, Xi'an 710072, PR China. Tel: +86 29 88492157; fax: +86 29 88460403.
E-mail addresses: dweifan@nwpu.edu.cn (Z.C. Deng), tjlu@mail.xjtu.edu.cn (T.J. Lu).

0022-5096/$ - see front matter © 2007 Published by Elsevier Ltd.
doi:10.1016/j.jmps.2007.04.007

length is preferred for enhanced thermo-mechanical performance, the influence of the outer radius of the cylinder is rather weak.

Keywords: Cellular materials; Pressurized hollow cylinder; Sandwich wall; Active cooling; Optimal design; Minimum mass; Multifunction

1. Introduction

All metallic sandwich panels with open, periodic cellular cores have recently emerged as one of the most weight efficient structures, such as three-dimensional (3D) truss cores and two-dimensional (2D) prismatic cores; see, for example, Hutchinson and He (2000), Wicks and Hutchinson (2001), Valdevit et al. (2004, 2006a, b), and Liu et al. (2006). Concomitantly, the open core topologies provide access for multifunctional applications, such as simultaneous load bearing and active cooling (Kim et al., 2004; Tian et al., 2004; Lu et al., 2005; Raskie, 2006); blast resistance (Xue and Hutchinson, 2003, 2006); vibration and noise control (Lu et al., 2000; Ruzzene, 2004); and structural actuation (Hutchinson et al., 2003; Wicks and Hutchinson, 2004).

Prior work has tended to focus on applications involving dynamic shock-type loadings, and for that class of problems the benefits of sandwich construction have been well established. Recently, a statically loaded cylindrical shell with sandwich walls subjected to internal pressure loading has been optimized by Liu et al. (2006). Five different core topologies are considered: Kagomé truss, single-layered pyramidal truss, double-layered pyramidal truss, single-layered corrugated core and double-layered corrugated core. Note that the deformation of most of these structures is governed by cell wall/ligament stretching, as opposed to bending commonly found in stochastic metal foams. Although the problem considered by Liu et al. (2006) is well-known to be not bending dominated, their results clearly demonstrate the significant benefit from sandwich construction relative to hollow cylinders having monolithic walls, which is interesting and intriguing.

Built upon the work of Liu et al. (2006), the study presented in this paper focuses on the bi-functional performances of 2D cellular metallic cores, namely, hollow sandwich cylinders subjected to a combination of internal pressure and thermal loading are optimized. Potential applications include cylindrical combustion chambers for rocket and missile propulsion, as well as airplane and land-based vehicle engines with the use of turbines and pistons (Raskie, 2006).

Combustion chambers are traditionally enclosed in monolithic structures that must withstand the high pressures and temperatures of combustion. A combustion engine that is both structurally lighter and more efficient in heat dissipation can significantly reduce weight and energy consumption (Raskie, 2006). It is anticipated here that using sandwich constructions with lightweight cellular topologies may improve the engine performance. Specifically, combining these topologies with current engine design in the form of a hollow sandwich-walled cylinder (as shown in Fig. 1) would greatly decrease weight while allowing for active air convection cooling across the open passages. The aim is to optimize the topological and geometric parameters of the sandwich construction for maximum bi-functional performance.

Please cite this article as: Liu, T., et al., Bi-functional optimization of actively cooled, pressurized hollow sandwich cylinders with prismatic..., J. Mech. Phys. Solids (2007), doi:10.1016/j.jmps.2007.04.007

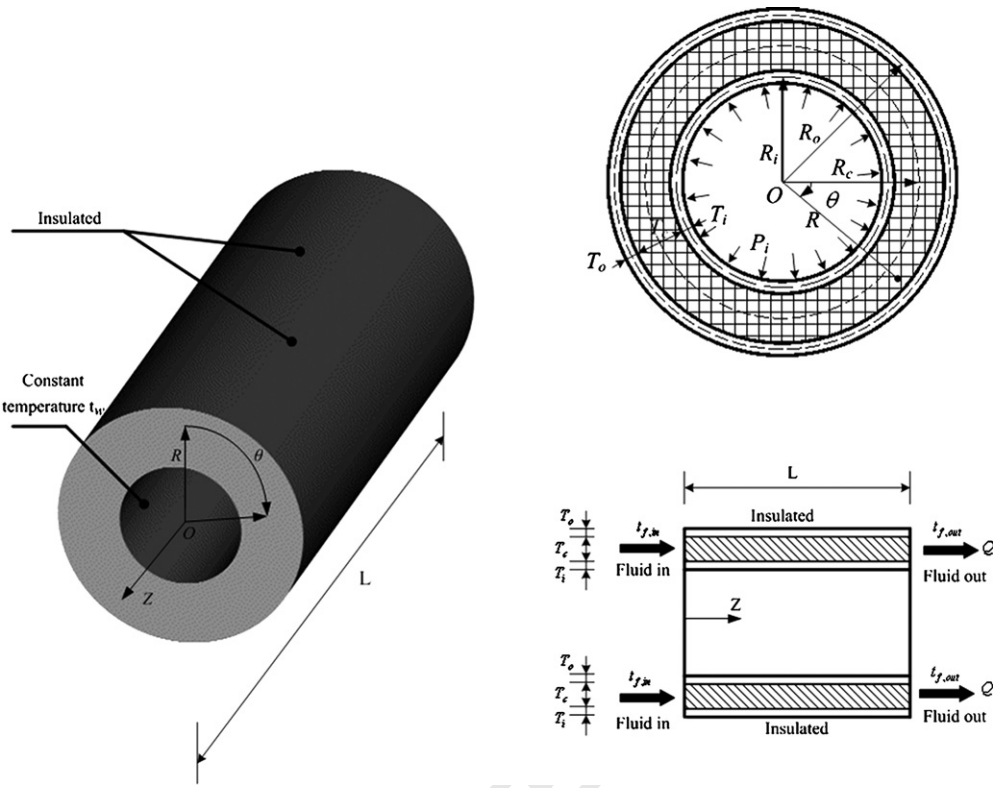

Fig. 1. Geometry of an internally pressurized hollow sandwich cylinder with inner facesheet kept isothermally and cooled by forced convection.

Two different prismatic core topologies are proposed for the hollow sandwich-walled cylinder, namely, square- and triangular-celled cores (see Fig. 2). The structural and thermal advantages of sandwich panels made with these 2D cellular materials have been separately addressed by Valdevit et al. (2004, 2006a, b) and by Lu et al. (2005). For minimum mass designs of the hollow cylinder under internal pressure loading, a structural model will be developed in a way different from that described in Liu et al. (2006). In their work, both 2D prismatic cores and 3D truss cores were considered, and the mechanics of the highly porous cellular materials was analyzed by a homogenization technique. This method allows the elastic behavior of essentially any core to be characterized by means of an effective stiffness matrix, thus allowing for a more unified treatment of the problem. In the present study, as opposed to the more complex framework of homogenization, a simpler and more traditional "member by member" structural approach will be employed to analyze the mechanics of 2D sandwich cylindrical walls.

For the thermal properties of sandwich structures having 2D cellular cores subjected to forced convection, previous work includes the evaluation and optimization of hexagonal honeycombs under forced convection by Lu (1998), simultaneously evaluation of the structural and heat transfer performance of 2D cellular metals by Gu et al. (2001), and optimal cooling performance of metallic sandwich panels with prismatic cores by Valdevit et al. (2006a, b). These studies are all concerned with sandwich panels and are based on the

Please cite this article as: Liu, T., et al., Bi-functional optimization of actively cooled, pressurized hollow sandwich cylinders with prismatic..., J. Mech. Phys. Solids (2007), doi:10.1016/j.jmps.2007.04.007

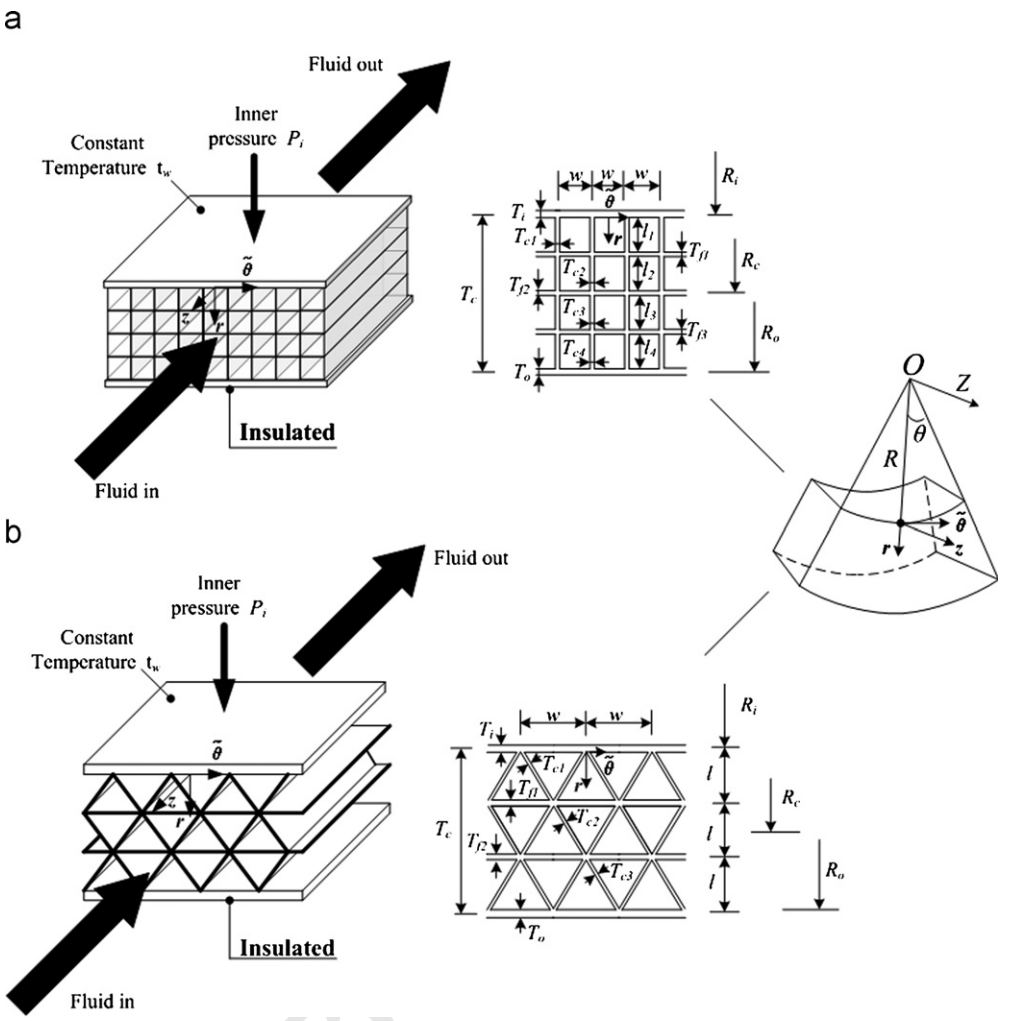

Fig. 2. 2D cellular metals considered in this paper: (a) square-celled core sandwich; (b) triangular-celled core sandwich.

assumption that the panel is sufficiently long to smooth out any entry and exit effects. In other words, fully developed flow profiles (both kinematical and thermal) are assumed. However, for a sandwich heat sink design with compact requirement (e.g., $L/D_h \leqslant 0.01\, Re_{D_h}$, where L and D_h are separately the length and hydraulic diameter of the sandwich core, and Re is the Reynolds number; see Fig. 1), developing flow and temperature fields are expected to prevail, thus significantly affecting its overall thermal performance.

In the present study, with the assumption that the flow is laminar in the 2D core passages, an approximate model incorporating the effects of developing flow and temperature fields will be established using the *intersection of asymptotes method*, and employed to analyze the thermal behavior of a sandwich-walled hollow cylinder (the inner

Please cite this article as: Liu, T., et al., Bi-functional optimization of actively cooled, pressurized hollow sandwich cylinders with prismatic..., J. Mech. Phys. Solids (2007), doi:10.1016/j.jmps.2007.04.007

surface of which is kept isothermally). Similar work on developing flow and temperature fields has been presented by Bejan and Sciubba (1992), in which the intersection of asymptotes method was first developed to optimize the plate spacing for an array of parallel plates cooled by forced convection. Later, Yilmaz et al. (2000) and Muzychka and Yovanovich (2004) separately applied this method to optimize the geometry of a single duct and 2D cellular metals at constant wall temperature, both cooled by forced laminar flow. More recently, for 2D cellular metals having either square or equilateral triangular cells, Wen et al. (2007) modified the approach of Muzychka and Yovanovich (2004) to account for the effect of solid conduction with the fin analogy model. In comparison with direct simulations using CFD (computational fluid dynamics), good predictions are obtained with the approximate but much simpler and computationally more efficient intersection of asymptotes method (Wen et al., 2007).

The article is organized as follows. In Section 2, the 2D topologies of sandwich cores are introduced. Sections 3 and 4 present the thermal model based on the intersection of asymptotes method and the structural model based on the member-by-member approach, respectively. The characteristics of optimization results obtained using either the thermal or structural model alone are analyzed. Section 5 introduces the thermo-mechanical joint optimization model, which uses a non-dimensional parameter to couple the two objectives (both structural and thermal) in a single cost function. As an example, an all metallic hollow sandwich cylinder subjected to simultaneous structural loading and active cooling is optimized using all the three models, and the results are compared. Section 6 discusses in detail the effects of geometrical parameters on the optimal structural parameters. Section 7 closes the paper with conclusions.

2. Definition of problem

2.1. The problem

Consider an all metallic, hollow, sandwich-walled cylinder subjected to a uniform internal pressure, P_i, and cooled by laminar forced convection, as shown in Fig. 1. The inner wall of the cylinder is kept isothermally and the sandwich has a lightweight 2D cellular core. The solid facesheets of the sandwich may have different thicknesses denoted here by T_i and T_o. Let T_c represent the total thickness of the sandwich core. Throughout the paper, subscripts i, o and c denote the inner facesheet, outer facesheet and core, respectively. In cylindrical polar coordinates (R, θ, Z), with the origin fixed at the center O of the cross-section of the cylinder (see Fig. 1), the radius of the centroidal surface of the inner facesheet, outer facesheet and core is represented separately as R_i, R_o and R_c. The goal is to optimize the sandwich geometry of the cylinder for maximum thermo-mechanical performance at minimum mass.

2.2. Topology of cellular core

The highly porous 2D cellular topologies concerned in the paper are shown in Fig. 2(a) for square-celled core and Fig. 2(b) for triangular-celled core. In both cases, the dimensions of core members are allowed to vary according to the stress gradient in the core, so that the sandwich-walled cylinder can be optimally designed as a minimum mass structure. Consequently, the cells shown in Fig. 2(a) are strictly speaking not square but

Please cite this article as: Liu, T., et al., Bi-functional optimization of actively cooled, pressurized hollow sandwich cylinders with prismatic..., J. Mech. Phys. Solids (2007), doi:10.1016/j.jmps.2007.04.007

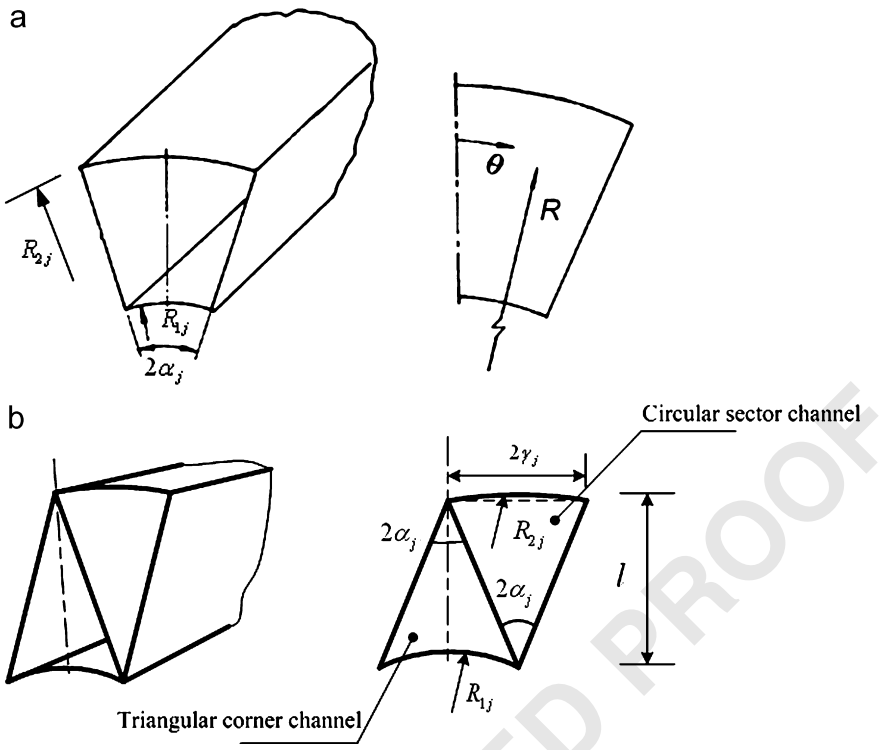

Fig. 3. Geometry of a unit channel for: (a) square-celled core sandwich; (b) triangular-celled core sandwich.

trapezoidal shaped, as shown in Fig. 3(a), with straight walls along the radial direction and curved walls along the circumferential direction. Similarly, the "triangular" cells shown in Fig. 3(b) have straight walls in the radial direction and curved walls in the circumferential direction. For convenience, unless otherwise stated, the trapezoidal shaped cells of Fig. 3(a) are termed "square cells" and the triangular-like cells of Fig. 3(b) are called "triangular cells" in this paper.

For the square-celled core of Fig. 2(a), T_{cj} and l_j $(j = 1, \ldots, n)$ denote the thickness and length of radial core members in the jth layer; T_{fk} $(k = 1, \ldots, n-1)$ denote the thickness of circumferential core members; w is the inner width of cells in the first layer of the core. For the triangular-celled core of Fig. 2(b), T_{cj} and T_{fk} denote the thickness of inclined and circumferential core members, respectively; w is the inner width of cells in the first layer of the core; l stands for the uniform thickness of each layer of the core. As also shown in Fig. 3, the cross-section of a channel in the square-celled core is an annular sector with net flow area A_{aj} (Fig. 3a), whereas, for the two kinds of channels in the triangular-celled core (Fig. 3b), the cross-sections are approximately circular sector with net flow area A_{cj} and triangular corner with net flow area A_{tj}, respectively. In the following sections, all these geometric parameters will act as design variables for optimization.

Based on the cellular geometry defined above for both topologies, the porosity ξ, defined as the ratio of void volume in the core to total volume of the core, can be written as

Please cite this article as: Liu, T., et al., Bi-functional optimization of actively cooled, pressurized hollow sandwich cylinders with prismatic..., J. Mech. Phys. Solids (2007), doi:10.1016/j.jmps.2007.04.007

$$\xi = \frac{\sum_{j=1}^{n} S_j \xi_j}{\sum_{j=1}^{n} S_j} = \frac{\sum_{j=1}^{n} N_j A_j}{\sum_{j=1}^{n} S_j}, \tag{1}$$

where ξ_j and S_j are the porosity and total volume per unit length for the jth layer of the core; N_j and A_j are the total number of channels and net flow area of a unit channel (as defined in Fig. 3) in the jth layer of the core. One has $N_1 = N_2 = \cdots \equiv \widetilde{N}$, $A_j = A_{aj}$ (annular-sector channel) or $A_j = A_{cj} + A_{tj}$ (circular sector and triangular corner channels).

3. Thermal analysis

As shown in Fig. 1, the 2D sandwich-walled hollow cylinder with inner substrate kept isothermally at temperature t_w and outer substrate thermally insulated is cooled by a coolant fluid having inlet temperature $t_{f,in}(< t_w)$ and driven in by pumping power $\widehat{P}$. It is assumed that all the cells are subjected to the same pressure drop $\Delta\widehat{p}$ over the entire length L of the cylinder, thus allowing channels in different layers of the core to experience different flow velocities. Let U_m and U_{mj} denote separately the mean fluid velocity upstream of the core and that for the jth layer of the core, and let U_j denote the mean fluid velocity in a unit channel of the jth layer. By mass conservation and momentum conservation, we have:

$$U_m = \frac{\sum_{j=1}^{n} S_j U_{mj}}{\sum_{j=1}^{n} S_j} = \frac{\sum_{j=1}^{n} S_j \xi_j U_j}{\sum_{j=1}^{n} S_j} = \frac{\widetilde{N}\sum_{j=1}^{n} A_j U_j}{\sum_{j=1}^{n} S_j}, \quad U_{mj} = \xi_j U_j, \tag{2}$$

$$\widehat{P} = \Delta\widehat{p} U_m \sum_{j=1}^{n} S_j, \tag{3}$$

where

$$\sum_{j=1}^{n} S_j = \pi[(R_o - T_o/2)^2 - (R_i + T_i/2)^2], \quad U_j = U_{a,j}$$

for the square-celled core, and

$$U_j = \frac{A_{cj}}{A_j} U_{c,j} + \frac{A_{tj}}{A_j} U_{t,j}$$

for the triangular-celled core.

The aim of thermal design for a sandwich cylinder is to maximize the total amount of heat dissipation at a fixed pumping power. Following Wen et al. (2007), the intersection of asymptotes method originally developed by Bejan and Sciubba (1992) is adopted to account for the entry and exit effects that are significant in a 2D honeycomb-type compact heat exchanger like the one shown in Fig. 1. Note that, whilst Wen et al. (2007) only studied the thermal performance of square and equilateral triangular cells in flat sandwich panels, the cell topologies addressed in this paper is more complicated, as seen in Figs. 3(a) and (b).

Please cite this article as: Liu, T., et al., Bi-functional optimization of actively cooled, pressurized hollow sandwich cylinders with prismatic..., J. Mech. Phys. Solids (2007), doi:10.1016/j.jmps.2007.04.007

3.1. Limit I: fully developed case

Consider first the limit, $L \to \infty$ (or, equivalently, the hydraulic diameter of a channel $D_h \to 0$), wherein each channel is slender enough so that the flow is fully developed and the fluid outlet temperature approaches t_w. Hence, the total amount of heat dissipated by the cylindrical sandwich heat sink is given by

$$Q_I = \rho_f c_p U_m (t_w - t_{f,in}) \sum_{j=1}^{n} S_j = \rho_f c_p \widetilde{N} (t_w - t_{f,in}) \sum_{j=1}^{n} A_j U_j = \sum_{j=1}^{n} Q_{I,j}, \tag{4}$$

where ρ_f and c_p are density and specific heat of the coolant, respectively, $Q_{I,j}$ is the total heat transfer rate of the channels in the jth layer:

$$Q_{I,j} = \rho_f c_p (t_w - t_{f,in}) \widetilde{N} A_j U_j = \rho_f c_p (t_w - t_{f,in}) U_{mj} S_j. \tag{5}$$

For fully developed flow in a 2D channel, the pressure drop is

$$f_j \, Re_{D_h,j} = 64 \Psi_j, \tag{6}$$

where

$$f_j = \frac{\Delta \widehat{p}}{L} \frac{D_{hj}}{\rho_f U_j^2/2}, \tag{7}$$

$$Re_{D_h,j} = \frac{U_j D_{hj}}{v_f}. \tag{8}$$

Here, f_j, D_{hj} and Ψ_j are the friction factor, hydraulic diameter and shape factor for channels in the jth layer, respectively, v_f is the kinematic viscosity of the coolant, and Re_{D_h} is Reynolds number based on D_h. Muzychka and Yovanovich (2002) demonstrated that when the friction factor and Reynolds number are based on the square root of the cross-sectional area of a 2D duct, the vast number of existing data for many channel shapes were reduced to a single curve which was merely a function of the aspect ratio of the duct or channel. They also showed that this curve was accurately represented by the first term of the exact series solution for the rectangular channel cross-section, given by

$$f \, Re_{\sqrt{A},j} = \frac{12}{\sqrt{\widetilde{\varepsilon}_j}(1+\widetilde{\varepsilon}_j)\left[1 - \dfrac{192\widetilde{\varepsilon}_j}{\pi^5} \tanh\left(\dfrac{\pi}{2\widetilde{\varepsilon}_j}\right)\right]}. \tag{9}$$

Here,

$$f \, Re_{\sqrt{A},j} = f \, Re_{D_h,j} \times \frac{\widetilde{C}_j}{16\sqrt{A_j}}, \tag{10}$$

where $\widetilde{C}_j$ and $\widetilde{\varepsilon}_j$ are the perimeter and aspect ratio of a cell in the jth layer. For the annular-sector channel and circular-sector channel shown in Figs. 3(a) and (b), $\widetilde{\varepsilon}_j$ can be defined as

$$\widetilde{\varepsilon}_j = \frac{(R_{2j} - R_{1j})}{(R_{1j} + R_{2j})\alpha_j} \quad \text{(Annular-sector channel in the } j\text{th layer)}, \tag{11}$$

Please cite this article as: Liu, T., et al., Bi-functional optimization of actively cooled, pressurized hollow sandwich cylinders with prismatic..., J. Mech. Phys. Solids (2007), doi:10.1016/j.jmps.2007.04.007

$$\widetilde{\varepsilon}_j = \frac{l}{2\gamma_j} \quad \text{(Circular-sector channel in the } j\text{th layer)}, \tag{12}$$

where R_{1j}, R_{2j}, α_j and γ_j denote the inner radius, outer radius, apex angle and chord length of the channel (Fig. 3). For the triangular corner channel of Fig. 3(b), the value of $f\,Re_{\sqrt{A}}$ is approximately equal to that of the circular channel (Muzychka and Yovanovich, 2004, 2002), namely, $f\,Re_{\sqrt{A}} = 14.18$. Hence, we have:

$$\Psi_{\beta j} = \frac{3\sqrt{A_{\beta j}}}{\sqrt{\widetilde{\varepsilon}}(1+\widetilde{\varepsilon})\left[1 - \dfrac{192\widetilde{\varepsilon}}{\pi^5}\tanh\left(\dfrac{\pi}{2\widetilde{\varepsilon}}\right)\right]\widetilde{C}_j}, \quad (\beta = a, c) \tag{13}$$

for annular-sector channel ($\beta = a$) and circular sector channel ($\beta = c$) in the jth layer, and

$$\Psi_{tj} = \frac{7.09\sqrt{A_{tj}}}{2\widetilde{C}_j} \tag{14}$$

for triangular corner channel in the jth layer.

From Eqs. (2), (3), (6)–(8), we obtain for square cells

$$U_m = \left\{\frac{\widehat{P}\widetilde{N}}{[\sum_{j=1}^{n} S_j]^2 \rho_f v_f L}\right\}^{1/2} \sqrt{\sum_{j=1}^{n}\left(\frac{D_{h,aj}^2 A_{aj}}{32\Psi_{aj}}\right)}, \tag{15}$$

$$U_j = \left(\frac{\widehat{P}}{\rho_f v_f L\widetilde{N}}\right)^{1/2} \frac{D_{hj}^2}{32\Psi_{aj}} \frac{1}{\sqrt{\sum_{j=1}^{n}\left(\dfrac{D_{h,aj}^2 A_{aj}}{32\Psi_{aj}}\right)}} \tag{16}$$

and, for triangular cells

$$U_m = \left\{\frac{\widehat{P}\widetilde{N}}{[\sum_{j=1}^{n} S_j]^2 \rho_f v_f L}\right\}^{1/2} \sqrt{\sum_{j=1}^{n}\left(\frac{D_{h,cj}^2 A_{cj}}{32\Psi_{cj}} + \frac{D_{h,tj}^2 A_{tj}}{32\Psi_{tj}}\right)}, \tag{17}$$

$$U_j = \frac{\left(\dfrac{\widehat{P}}{\rho_f v_f L\widetilde{N}}\right)^{1/2}\left[A_{cj}\dfrac{D_{h,cj}^2}{\Psi_{cj}} + A_{tj}\dfrac{D_{h,tj}^2}{\Psi_{tj}}\right]}{32A_j\sqrt{\sum_{j=1}^{n}\left(\dfrac{D_{h,cj}^2 A_{cj}}{32\Psi_{cj}} + \dfrac{D_{h,tj}^2 A_{tj}}{32\Psi_{tj}}\right)}}. \tag{18}$$

Hence, at the panel level we have

$$Q_1 = c_p \rho_f^{1/2}\left(\frac{\widehat{P}\widetilde{N}}{v_f L}\right)^{1/2} \sqrt{\sum_{j=1}^{n}\left(\frac{D_{h,aj}^2 A_{aj}}{32\Psi_{aj}}\right)}(t_w - t_{f,in})$$

(Square-celled core sandwich cylinder) (19)

Please cite this article as: Liu, T., et al., Bi-functional optimization of actively cooled, pressurized hollow sandwich cylinders with prismatic..., J. Mech. Phys. Solids (2007), doi:10.1016/j.jmps.2007.04.007

$$Q_{\mathrm{I}} = c_p \rho_f^{1/2} \left(\frac{\widehat{P}\widetilde{N}}{v_f L}\right)^{1/2} \sqrt{\sum_{j=1}^{n} \left(\frac{D_{\mathrm{h,c}j}^2 A_{\mathrm{c}j}}{32\Psi_{\mathrm{c}j}} + \frac{D_{\mathrm{h,t}j}^2 A_{\mathrm{t}j}}{32\Psi_{\mathrm{t}j}}\right)} (t_{\mathrm{w}} - t_{\mathrm{f,in}})$$

(Triangular-celled core sandwich cylinder), (20)

whereas at the channel level we have

$$Q_{\mathrm{I},j} = c_p \rho_f^{1/2} \left(\frac{\widehat{P}\widetilde{N}}{v_f L}\right)^{1/2} \frac{D_{\mathrm{h,a}j}^2 A_{\mathrm{a}j}}{32\Psi_{\mathrm{a}j}} \frac{1}{\sqrt{\sum_{j=1}^{n} \left(\frac{D_{\mathrm{h,a}j}^2 A_{\mathrm{a}j}}{32\Psi_{\mathrm{a}j}}\right)}} (t_{\mathrm{w}} - t_{\mathrm{f,in}})$$

(Square-celled core sandwich cylinder), (21)

$$Q_{\mathrm{I},j} = c_p \rho_f^{1/2} \left(\frac{\widehat{P}\widetilde{N}}{v_f L}\right)^{1/2} \frac{\left[A_{\mathrm{c}j}\frac{D_{\mathrm{h,c}j}^2}{\Psi_{\mathrm{c}j}} + A_{\mathrm{t}j}\frac{D_{\mathrm{h,t}j}^2}{\Psi_{\mathrm{t}j}}\right]}{32\sqrt{\sum_{j=1}^{n} \left(\frac{D_{\mathrm{h,c}j}^2 A_{\mathrm{c}j}}{32\Psi_{\mathrm{c}j}} + \frac{D_{\mathrm{h,t}j}^2 A_{\mathrm{t}j}}{32\Psi_{\mathrm{t}j}}\right)}} (t_{\mathrm{w}} - t_{\mathrm{f,in}})$$

(Triangular-celled core sandwich cylinder). (22)

Given that $\widetilde{N} \sim \pi[R_{2j}^2 - R_{1j}^2]/D_{\mathrm{h}j}^2$, it can be shown that the heat transfer rate at either the panel or channel level, given separately by Eqs. (4) and (5), has the following dependency: Q_{I}, $Q_{\mathrm{I},j} \sim D_{\mathrm{h}j}/L^{1/2}$.

3.2. Limit II: boundary layer case

In the opposite extreme, $D_{\mathrm{h}} \to \infty$ or $L \to 0$, the fluid flow and heat transfer can be approximated using boundary layer theory (Bejan and Sciubba, 1992). The L-averaged wall shear stress τ reads:

$$\tau_j = 1.328(\rho_f U_j^2/2)\, Re_L^{-1/2} = \frac{\Delta\widehat{p}}{L}\frac{D_{\mathrm{h}j}}{4}, \tag{23}$$

where

$$Re_L = \frac{U_j L}{v_f}. \tag{24}$$

Hence, for a square-celled core sandwich cylinder

$$U_j = \left(0.557 \frac{\widehat{P}^{3/5} D_{\mathrm{h,a}j}}{v_f^{3/10} L^{3/10} \rho_f^{3/5} \widetilde{N}^{3/5} (\sum_{j=1}^{n} A_{\mathrm{a}j} D_{\mathrm{h,a}j}^{2/3})^{3/5}}\right)^{2/3}, \tag{25}$$

$$U_{\mathrm{m}} = \left(0.677 \frac{\widehat{P}^{2/5} \widetilde{N}^{3/5}}{v_f^{1/5} L^{1/5} \rho_f^{2/5} \sum_{j=1}^{n} S_j}\right) \left(\sum_{j=1}^{n} A_{\mathrm{a}j} D_{\mathrm{h,a}j}^{2/3}\right)^{3/5} \tag{26}$$

and, for a triangular-celled core sandwich cylinder

Please cite this article as: Liu, T., et al., Bi-functional optimization of actively cooled, pressurized hollow sandwich cylinders with prismatic..., J. Mech. Phys. Solids (2007), doi:10.1016/j.jmps.2007.04.007

$$U_j = \left(\frac{0.557}{v_f^{3/10} L^{3/10} \rho_f^{3/5} \widetilde{N}^{3/5} (\sum_{j=1}^{n} (A_{cj} D_{h,cj}^{2/3} + A_{tj} D_{h,tj}^{2/3}))^{3/5}}\right)^{2/3} \left(\frac{A_{cj}}{A_j} D_{h,cj}^{2/3} + \frac{A_{tj}}{A_j} D_{h,tj}^{2/3}\right) \widehat{P}^{2/5}, \tag{27}$$

$$U_m = \left(0.677 \frac{\widehat{P}^{2/5} \widetilde{N}^{3/5}}{v_f^{1/5} L^{1/5} \rho_f^{2/5} \sum_{j=1}^{n} S_j}\right) \left(\sum_{j=1}^{n} (A_{cj} D_{h,cj}^{2/3} + A_{tj} D_{h,tj}^{2/3})\right)^{3/5}. \tag{28}$$

The local and global heat transfer coefficients for channels in the jth layer, $h_j(z)$ and $\overline{h}_j(z)$, can be calculated as (Bejan and Sciubba, 1992; Wen et al., 2007)

$$h_j(z) = Nu(z) \frac{k_f}{z} = 0.332 k_f \, Pr^{1/3} \left(\frac{U_j}{z v_f}\right)^{1/2}, \tag{29}$$

$$\overline{h}_j(z) = \overline{Nu}(z) \frac{k_f}{z} = 0.664 k_f \, Pr^{1/3} \left(\frac{U_j}{z v_f}\right)^{1/2}, \tag{30}$$

where Pr and k_f are Prandtl number and thermal conductivity of the coolant, respectively. Therefore, for heat transfer in boundary layers along a flat plate having arbitrary temperature, the local heat flux is obtained as

$$\widetilde{q}(z) = h(z) \int_0^z \frac{\mathrm{d}t_w(\eta)}{[1 - (\eta/z)^{3/4}]^{1/3}} \, \mathrm{d}\eta + h(z)[t_w(0) - t_{f,in}], \tag{31}$$

where $h(z)$ can be approximated as the weighted average of the channel values in different layers, i.e., $h(z) = \sum_{j=1}^{n} [(S_j \xi_j h_j(z))/(\xi \sum_{j=1}^{n} S_j)]$.

If the thermal conduction resistance in solid walls is ignored (i.e., $k_s \to \infty$), we have

$$Q_{II,j} = L \widetilde{N} \overline{h}_{j,L} \widetilde{C}_j (t_w - t_{f,in}), \quad Q_{II} = L \widetilde{N} \sum_{j=1}^{n} \overline{h}_{j,L} \widetilde{C}_j (t_w - t_{f,in}). \tag{32}$$

Hence, at the panel level

$$Q_{II} = \frac{0.5463 \widetilde{N}^{4/5} k_f \, Pr^{1/3} \widehat{P}^{1/5} L^{2/5}}{v_f^{3/5} \rho_f^{1/5} (\sum_{j=1}^{n} A_{aj} D_{h,aj}^{2/3})^{1/5}} \sum_{j=1}^{n} (\widetilde{C}_{aj} D_{h,aj}^{1/3})(t_w - t_{f,in})$$

(Square-celled core sandwich cylinder), (33)

$$Q_{II} = \frac{0.5463 \widetilde{N}^{4/5} k_f \, Pr^{1/3} \widehat{P}^{1/5} L^{2/5}}{v_f^{3/5} \rho_f^{1/5} (\sum_{j=1}^{n} (A_{cj} D_{h,cj}^{2/3} + A_{tj} D_{h,tj}^{2/3}))^{1/5}} \times \sum_{j=1}^{n} \left[(\widetilde{C}_{cj} + \widetilde{C}_{tj}) \left(\frac{A_{cj}}{A_j} D_{h,cj}^{2/3} + \frac{A_{tj}}{A_j} D_{h,tj}^{2/3}\right)^{1/2} \right] (t_w - t_{f,in})$$

(Triangular-celled core sandwich cylinder) (34)

and, at the channel level

Please cite this article as: Liu, T., et al., Bi-functional optimization of actively cooled, pressurized hollow sandwich cylinders with prismatic..., J. Mech. Phys. Solids (2007), doi:10.1016/j.jmps.2007.04.007

$$Q_{\mathrm{II},j}=\frac{0.5463\widetilde{N}^{4/5}k_f\,Pr^{1/3}\widehat{P}^{1/5}L^{2/5}}{v_f^{3/5}\rho_f^{1/5}(\sum_{j=1}^{n}A_{\mathrm{a}j}D_{\mathrm{h,a}j}^{2/3})^{1/5}}\widetilde{C}_{\mathrm{a}j}D_{\mathrm{h,a}j}^{1/3}(t_{\mathrm{w}}-t_{\mathrm{f,in}})$$

(Square-celled core sandwich cylinder), (35)

$$Q_{\mathrm{II},j}=\frac{0.5463\widetilde{N}^{4/5}k_f\,Pr^{1/3}\widehat{P}^{1/5}L^{2/5}}{v_f^{3/5}\rho_f^{1/5}(\sum_{j=1}^{n}(A_{\mathrm{c}j}D_{\mathrm{h,c}j}^{2/3}+A_{\mathrm{t}j}D_{\mathrm{h,t}j}^{2/3}))^{1/5}}\times\left[(\widetilde{C}_{\mathrm{c}j}+\widetilde{C}_{\mathrm{t}j})\left(\frac{A_{\mathrm{c}j}}{A_j}D_{\mathrm{h,c}j}^{2/3}+\frac{A_{\mathrm{t}j}}{A_j}D_{\mathrm{h,t}j}^{2/3}\right)^{1/2}\right](t_{\mathrm{w}}-t_{\mathrm{f,in}})$$

(Triangular-celled core sandwich cylinder). (36)

In this case, it can be shown that the heat transfer rate at either the panel or channel level has the following dependency: Q_{II}, $Q_{\mathrm{II},j}\sim L^{2/5}/D_{\mathrm{h}j}^{4/5}$.

For finite values of k_{s}, the thermal conduction resistance in solid walls needs to be accounted for. To this end, the fin analogy model (Lu, 1998) is employed, in which a two-step analysis is used: (a) heat transfer in a corrugated wall without fins is firstly analyzed; (b) contribution from the fins is subsequently calculated and added to that in (a), see Fig. 4. For the first step, with Eq. (31), the variation of temperature $t_{\mathrm{s}}(\zeta,z)$ along the length of a single corrugated wall without fins (Figs. 4b and d) is governed by

$$\frac{\partial^2 t_{\mathrm{s}}(\zeta,z)}{\partial\zeta^2}-\frac{2h(z)}{k_{\mathrm{s}}\widetilde{T}_{\mathrm{c}}}\left[t_{\mathrm{s}}(\zeta,0)+\int_0^z\frac{\partial t_{\mathrm{s}}(\zeta,\eta)/\partial\eta}{[1-(\eta/z)^{3/4}]^{1/3}}\,\mathrm{d}\eta-t_{\mathrm{f,in}}\right]=0, \tag{37}$$

where $\widetilde{T}_{\mathrm{c}}=\sum_{j=1}^{n}[(S_j\xi_jT_{\mathrm{c}j})/(\xi\sum_{j=1}^{n}S_j)]$ is the weighted average thickness of a vertical/inclined core member and $\zeta=C_Hr$ is the local coordinate along the corrugated wall, with $\zeta=0$ coinciding with $r=0$ (Fig. 4). The tortuous coefficient $C_H=1$ for square-celled core and $C_H=1/\sin\phi$ for triangular-celled core, where ϕ is the inclination angle of the cell wall (Fig. 4c).

Following Wen et al. (2007), Eq. (37) can be approximately rewritten as

$$\frac{\partial^2 t_{\mathrm{s}}(\zeta,z)}{\partial\zeta^2}-\frac{2h(z)}{k_{\mathrm{s}}\widetilde{T}_{\mathrm{c}}}[t_{\mathrm{s}}(\zeta,z)-t_{\mathrm{f,in}}]=0. \tag{38}$$

Therefore, with the following boundary conditions

$$\begin{cases}t_{\mathrm{s}}=t_{\mathrm{w}}, & \zeta=0,\\ k_{\mathrm{s}}\dfrac{\partial t_{\mathrm{s}}}{\partial\zeta}=0, & \zeta=\zeta_H=C_H(h_{\mathrm{c}}-T_{\mathrm{i}}/2-T_{\mathrm{o}}/2)\end{cases} \tag{39}$$

the solution of (38) is given by

$$t_{\mathrm{s}}(\zeta,z)=t_{\mathrm{f,in}}+(t_{\mathrm{w}}-t_{\mathrm{f,in}})\frac{\cosh\left[\left(\sqrt{\dfrac{2h(z)}{k_{\mathrm{s}}\widetilde{T}_{\mathrm{c}}}}\right)(\zeta_H-\zeta)\right]}{\cosh\left(\left(\sqrt{\dfrac{2h(z)}{k_{\mathrm{s}}\widetilde{T}_{\mathrm{c}}}}\right)\zeta_H\right)}. \tag{40}$$

The total heat lost to the cooling medium per unit length of the corrugated wall is thence

Please cite this article as: Liu, T., et al., Bi-functional optimization of actively cooled, pressurized hollow sandwich cylinders with prismatic..., J. Mech. Phys. Solids (2007), doi:10.1016/j.jmps.2007.04.007

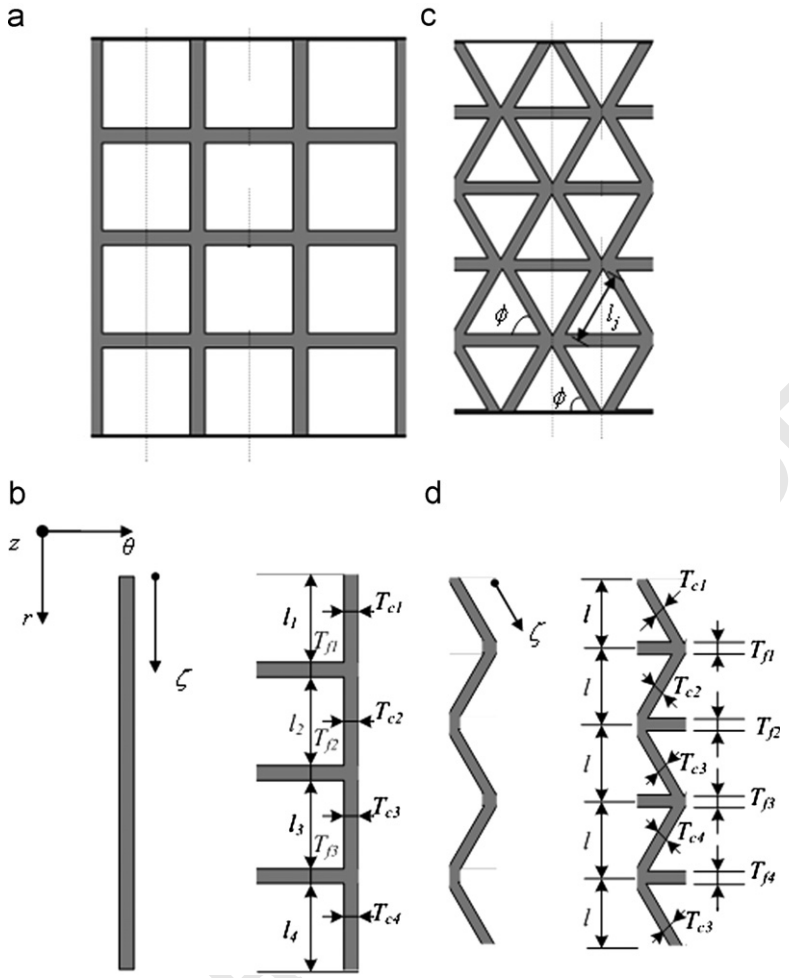

Fig. 4. Two step analysis with fin analogy model: (a) topology of square-celled core; (b) single-corrugated walls with and without fins for square cells; (c) topology of triangular-celled core; (d) single-corrugated walls with and without fins for triangular cells.

$$q_1(z) = -k_s \widetilde{T}_c \frac{\mathrm{d}t_s}{\mathrm{d}\zeta}\bigg|_{\zeta=0} = (t_w - t_{f,in})(\sqrt{2h(z)k_s\widetilde{T}_c}) \tanh\left[\left(\sqrt{\frac{2h(z)}{k_s\widetilde{T}_c}}\right)\zeta_H\right]. \tag{41}$$

In the second step, with the heat dissipated into the coolant from the fins and substrates both accounted for, the total heat transfer rate is given by

$$Q_{II} = \int_0^L [q(z) + q_{wi}(z) + q_{wo}(z)]\,\mathrm{d}z, \tag{42}$$

where

$$q(z) = \psi\widetilde{N}(1 + C_{fin})q_1(z), \tag{43}$$

Please cite this article as: Liu, T., et al., Bi-functional optimization of actively cooled, pressurized hollow sandwich cylinders with prismatic..., J. Mech. Phys. Solids (2007), doi:10.1016/j.jmps.2007.04.007

$$q_{\mathrm{wi}}(z) = h_1(z)[2\pi(R_{\mathrm{i}} + T_{\mathrm{i}}/2) - \psi\widetilde{N}C_H T_{\mathrm{c1}}](t_{\mathrm{w}} - t_{\mathrm{f,in}}), \tag{44}$$

$$\begin{aligned} q_{\mathrm{wo}}(z) &= h_n(z)[2\pi(R_{\mathrm{o}} - T_{\mathrm{o}}/2) - \psi\widetilde{N}C_H T_{cn}](t_{\mathrm{s}}(\zeta_H, z) - t_{\mathrm{f,in}}) \\ &= \frac{h_n(z)[2\pi(R_{\mathrm{o}} - T_{\mathrm{o}}/2) - \psi\widetilde{N}C_H T_{cn}]}{\cosh\left(\left(\sqrt{\dfrac{2h(z)}{k_{\mathrm{s}}\widetilde{T}_{\mathrm{c}}}}\right)\zeta_H\right)}(t_{\mathrm{w}} - t_{\mathrm{f,in}}) \end{aligned} \tag{45}$$

with $\psi = 1$ for square-celled core and $\psi = 2$ for triangular-celled core. In Eq. (43), C_{fin} denotes the weight coefficient of fins on heat loss, which can be estimated by the ratio of total surface area of the fins to that of the corrugated wall (Lu, 1998). In Eqs. (44) and (45), $q_{\mathrm{wi}}(z)$ and q_{wo} stand for the heat flux into the coolant from the inner substrate and outer substrate, respectively. In Wen et al. (2007), the contribution of q_{wo} is not explicitly calculated. However, since the influence of q_{wo} is significant in the present study, an explicit calculation is necessary.

3.3. Thermal design model: intersection of asymptotes

To a good approximation, the optimal channel size of the 2D prismatic core may be found by intersecting the two asymptotes obtained above (Bejan and Sciubba, 1992; Wen et al., 2007). The exact shape of the heat transfer rate curve against channel size may be found by using more accurate expressions of Shah and London (1978) for individual channel geometries. However, CFD simulations presented in Wen et al. (2007) confirm the validity of the approximate yet much simpler intersection-of-asymptotes method.

At the panel level, for $k_{\mathrm{s}} \to$ inf, intersecting Eqs. (19), (20) and (33), (34) or (42) gives

$$\begin{aligned} &c_p\rho_f^{1/2}\left(\frac{\widehat{P}\widetilde{N}}{v_f L}\right)^{1/2}\sqrt{\sum_{j=1}^{n}\left(\frac{D_{\mathrm{h},aj}^2 A_{\mathrm{a}j}}{32\Psi_{\mathrm{a}j}}\right)}(t_{\mathrm{w}} - t_{\mathrm{f,in}}) \\ &= \frac{0.5463\widetilde{N}^{4/5}k_f\, Pr^{1/3}\widehat{P}^{1/5}L^{2/5}}{v_f^{3/5}\rho_f^{1/5}(\sum_{j=1}^{n}A_{\mathrm{a}j}D_{\mathrm{h},aj}^{2/3})^{1/5}}\sum_{j=1}^{n}(\widetilde{C}_{\mathrm{a}j}D_{\mathrm{h},aj}^{1/3})(t_{\mathrm{w}} - t_{\mathrm{f,in}}) \\ &\quad \text{(Square-celled core sandwich cylinder),} \end{aligned} \tag{46}$$

$$\begin{aligned} &c_p\rho_f^{1/2}\left(\frac{\widehat{P}\widetilde{N}}{v_f L}\right)^{1/2}\sqrt{\sum_{j=1}^{n}\left(\frac{D_{\mathrm{h},cj}^2 A_{\mathrm{c}j}}{32\Psi_{\mathrm{c}j}} + \frac{D_{\mathrm{h},tj}^2 A_{\mathrm{t}j}}{32\Psi_{\mathrm{t}j}}\right)}(t_{\mathrm{w}} - t_{\mathrm{f,in}}) \\ &= \frac{0.5463\widetilde{N}^{4/5}k_f\, Pr^{1/3}\widehat{P}^{1/5}L^{2/5}}{v_f^{3/5}\rho_f^{1/5}(\sum_{j=1}^{n}(A_{\mathrm{c}j}D_{\mathrm{h},cj}^{2/3} + A_{\mathrm{t}j}D_{\mathrm{h},tj}^{2/3}))^{1/5}} \\ &\quad \times\sum_{j=1}^{n}\left[(\widetilde{C}_{\mathrm{c}j} + \widetilde{C}_{\mathrm{t}j})\left(\frac{A_{\mathrm{c}j}}{A_j}D_{\mathrm{h},cj}^{2/3} + \frac{A_{\mathrm{t}j}}{A_j}D_{\mathrm{h},tj}^{2/3}\right)^{1/2}\right](t_{\mathrm{w}} - t_{\mathrm{f,in}}) \\ &\quad \text{(Triangular-celled core sandwich cylinder).} \end{aligned} \tag{47}$$

Similarly, for $k_{\mathrm{s}} \ll$ inf, one has

Please cite this article as: Liu, T., et al., Bi-functional optimization of actively cooled, pressurized hollow sandwich cylinders with prismatic..., J. Mech. Phys. Solids (2007), doi:10.1016/j.jmps.2007.04.007

$$c_p\rho_f^{1/2}\left(\frac{\widehat{P}\widetilde{N}}{v_f L}\right)^{1/2}\sqrt{\sum_{j=1}^{n}\left(\frac{D_{\mathrm{h},aj}^2 A_{aj}}{32\Psi_{aj}}\right)}(t_w - t_{f,in}) = \int_0^L [q(z) + q_{wi}(z) + q_{wo}(z)]\,dz \quad \text{(Square-celled core sandwich cylinder)}, \tag{48}$$

$$c_p\rho_f^{1/2}\left(\frac{\widehat{P}\widetilde{N}}{v_f L}\right)^{1/2}\sqrt{\sum_{j=1}^{n}\left(\frac{D_{\mathrm{h},cj}^2 A_{cj}}{32\Psi_{cj}} + \frac{D_{\mathrm{h},tj}^2 A_{tj}}{32\Psi_{tj}}\right)}(t_w - t_{f,in}) = \int_0^L [q(z) + q_{wi}(z) + q_{wo}(z)]\,dz \quad \text{(Triangular-celled core sandwich cylinder)}. \tag{49}$$

Since A_j, D_{hj} and $\widetilde{C_j}$ are functions of geometric parameters of the sandwich core (as defined in Section 2.2), Eqs. (46)–(49) can be geometrically described as hyperplanes composed of these parameters, and the optimum must be located on these hyperplanes. Hence, the optimal core geometry for maximum heat dissipation can be found by using (46)–(49) as the constraints of optimization. The corresponding objective function is defined as:

Model I:

$$\mathbf{Max}\ \chi_1(\mathbf{\Lambda}) = \frac{Q_I/L}{R_o^{1/2}(t_w - t_{f,in})} = \frac{1}{\left(\frac{L}{R_o}\right)^{3/2}} c_p\rho_f^{1/2}\left(\frac{\widehat{P}\widetilde{N}}{v_f}\right)^{1/2}\sqrt{\sum_{j=1}^{n}\left(\frac{\left(\frac{D_{\mathrm{h},aj}}{R_o}\right)^2\left(\frac{A_{aj}}{R_o^2}\right)}{32\Psi_{aj}}\right)}$$

(Square-celled core sandwich cylinder), (50)

$$\mathbf{Max}\ \chi_1(\mathbf{\Lambda}) = \frac{Q_I/L}{R_o^{1/2}(t_w - t_{f,in})} = \frac{1}{\left(\frac{L}{R_o}\right)^{3/2}} c_p\rho_f^{1/2}\left(\frac{\widehat{P}\widetilde{N}}{v_f}\right)^{1/2}\sqrt{\sum_{j=1}^{n}\left(\frac{\left(\frac{D_{\mathrm{h},cj}}{R_o}\right)^2\left(\frac{A_{cj}}{R_o^2}\right)}{32\Psi_{cj}} + \frac{\left(\frac{D_{\mathrm{h},tj}}{R_o}\right)^2\left(\frac{A_{tj}}{R_o^2}\right)}{32\Psi_{tj}}\right)}$$

(Triangular-celled core sandwich cylinder), (51)

where Q_I/L denotes the heat transfer rate per unit length and $\mathbf{\Lambda}$ is a non-dimensional design variable vector defining the geometry of the cylindrical sandwich.

$$\mathbf{\Lambda} = \left[\frac{T_o}{R_o}, \frac{T_i}{R_o}, \frac{R_i}{R_o}, \frac{T_{cj}}{R_o}, \frac{l_j}{R_o}, \frac{T_{fk}}{R_o}, \frac{w}{R_o}\right]^T \quad (j = 1, \ldots, n; k = 1, \ldots, n-1),$$

(Square-celled core sandwich cylinder) (52)

Please cite this article as: Liu, T., et al., Bi-functional optimization of actively cooled, pressurized hollow sandwich cylinders with prismatic..., J. Mech. Phys. Solids (2007), doi:10.1016/j.jmps.2007.04.007

$$\mathbf{\Lambda} = \left[\frac{T_o}{R_o}, \frac{T_i}{R_o}, \frac{R_i}{R_o}, \frac{T_{cj}}{R_o}, \frac{l}{R_o}, \frac{T_{fk}}{R_o}, \frac{w}{R_o}\right]^T \quad (j = 1, \ldots, n; k = 1, \ldots, n-1)$$

(Triangular-celled core sandwich cylinder). (53)

The auxiliary function used to find the variables characterizing the maximum χ_1 design for Eq. (50) is given by

$$F(\mathbf{\Lambda}) = \frac{R_o^{1/2}(t_w - t_{f,in})}{Q_I/L} - \lambda_1(t_w - t_{f,in})\left[c_p \rho_f^{1/2}\left(\frac{\widehat{P}\widetilde{N}}{v_f L}\right)^{1/2}\sqrt{\sum_{j=1}^{n}\left(\frac{D_{h,aj}^2 A_{aj}}{32\Psi_{aj}}\right)}\right.$$
$$\left. - \frac{0.5463\widetilde{N}^{4/5} k_f\, Pr^{1/3}\widehat{P}^{1/5} L^{2/5}}{v_f^{3/5}\rho_f^{1/5}(\sum_{j=1}^{n} A_{aj} D_{h,aj}^{2/3})^{1/5}}\sum_{j=1}^{n}(\widetilde{C}_{aj} D_{h,aj}^{1/3})\right], \quad (54)$$

where λ_1 is the Lagrangian multiplier. As mentioned above, A_j, D_{hj} and $\widetilde{C}_j$ are functions of $\mathbf{\Lambda}$. Hence, provided that L and R_o are fixed, according to Lagrange's multiplier theorem, it has been established that, in most cases, the solution of (50) is not unique; the same holds for (51). That is to say, the maximum value of $Q_I/L/R_o^{1/2}(t_w - t_{f,in})$ may be associated with a number of different sandwich designs. For the optimization problem associated with geometrical constraints described below in Sections 4–6, the same conclusion can be drawn by invoking the Kuhn–Tucker condition.

4. Minimum mass design optimization

The minimum weights of an internally pressurized hollow sandwich cylinder with either 3D truss core or 2D corrugated core have been reported by Liu et al. (2006). For the structural analysis of a sandwich cylinder as shown in Fig. 1, they adopted an approach whereby the cellular core was firstly homogenized into a 3D anisotropic elastic continuum and then, built upon the works of Timoshenko and Young (1956) and Lekhniĕtìskiæi (1981), closed form elastic solutions were employed to predict the responses of structural members of the sandwich. Comparisons with finite element method (FEM) results suggest that the behaviors of both corrugated and truss core sandwiches can be predictably well by the homogenization approach. In other words, various sandwich theories, which are the approximation of classical solutions, can be employed to predict the behaviors of engineering structures made with cellular materials. As also revealed by the homogenization approach, for monoclinic core or general anisotropic core sandwich cylinders, the stress distribution in the structure is complex, e.g., torsional deformation of facesheets may be induced by the anisotropy of cores, whereas, for orthotropic cores (as the prismatic cores in this paper), the stress distribution is simpler (as described in Section 4.1). In this paper, since our interest mainly focuses on the thermo-mechanical optimization of a hollow sandwich cylinder with orthotropic core, to make it simple, a more direct and simpler structural method is used, as described below.

4.1. Structural analysis

Consider the unit cell of a square- or triangular-celled core sandwich, each having a single layer, as shown in Figs. 5(a) and (b); the corresponding face-core interfacial stresses,

Please cite this article as: Liu, T., et al., Bi-functional optimization of actively cooled, pressurized hollow sandwich cylinders with prismatic..., J. Mech. Phys. Solids (2007), doi:10.1016/j.jmps.2007.04.007

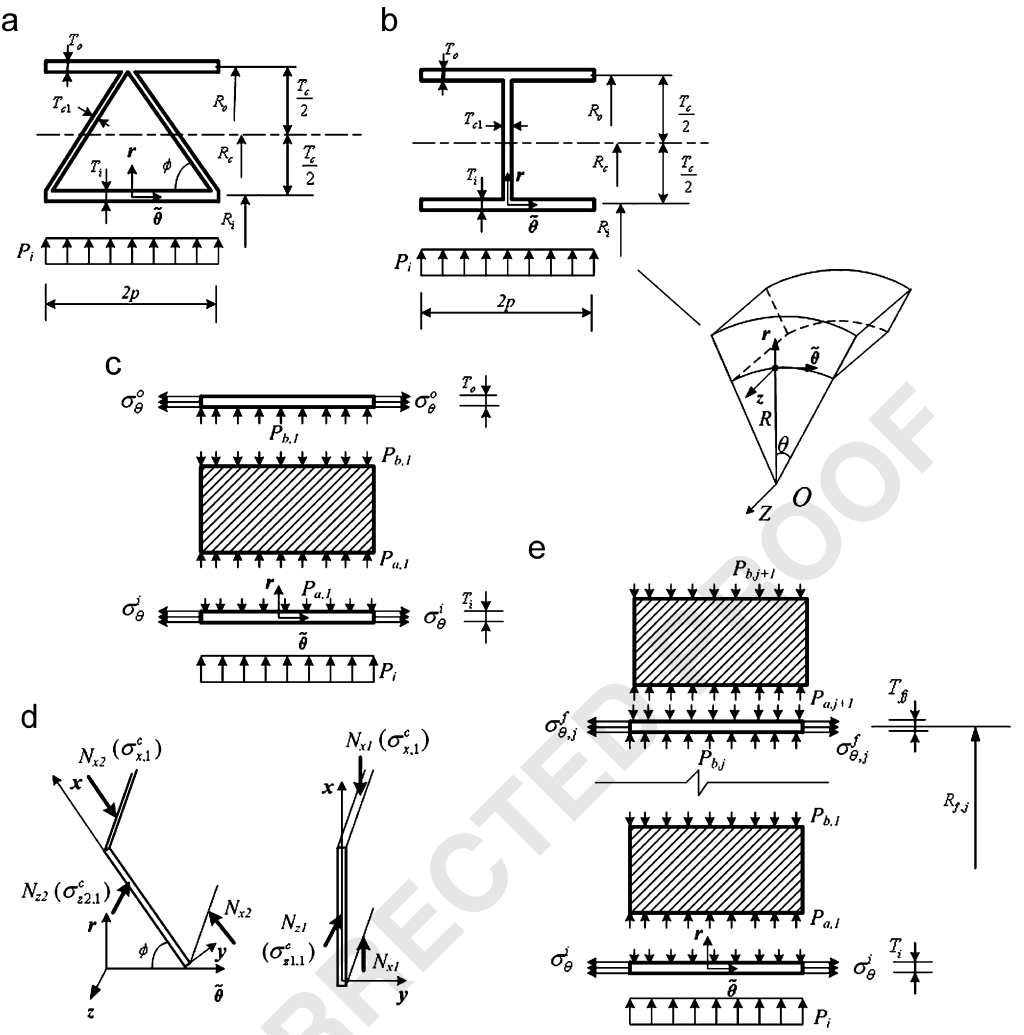

Fig. 5. Unit cell of single- or multilayered sandwich with: (a) square cells and (b) triangular cells; (c) stresses in the core and facesheets of single-layered sandwich; (d) stresses in core members; (e) stresses in the core and facesheets of a multilayered sandwich.

$P_{a,1}$ and $P_{b,1}$, are shown in Fig. 5(c), provided that the cellular core is treated as a 3D orthotropic elastic continuum. According to Liu et al. (2006), if the core is orthotropic, only normal stresses within the two interfaces exist, and the core members are dominated by membrane forces as shown in Fig. 5(d). It is assumed that the sandwich cylinder concerned is without end caps and fixed at both ends. Hence, the generalized plane deformation assumption is adopted, namely, not only the stresses, but also the displacements, do not depend on the axial coordinate (z). Therefore, the outer facesheet is subjected to an internal pressure whilst the inner facesheet is subjected to both internal and external pressures (see Fig. 5c). With the Lamé equations (Timoshenko and Young, 1956), the planar elastic stresses of the inner facesheet are:

Please cite this article as: Liu, T., et al., Bi-functional optimization of actively cooled, pressurized hollow sandwich cylinders with prismatic..., J. Mech. Phys. Solids (2007), doi:10.1016/j.jmps.2007.04.007

$$\sigma_R^{\mathrm{i}} = -\frac{\dfrac{(R_{\mathrm{i}}+T_{\mathrm{i}}/2)^2}{R^2}-1}{\dfrac{(R_{\mathrm{i}}+T_{\mathrm{i}}/2)^2}{(R_{\mathrm{i}}-T_{\mathrm{i}})^2}-1}P_i - \frac{1-\dfrac{(R_{\mathrm{i}}-T_{\mathrm{i}}/2)^2}{R^2}}{1-\dfrac{(R_{\mathrm{i}}-T_{\mathrm{i}}/2)^2}{(R_{\mathrm{i}}+T_{\mathrm{i}}/2)^2}}(-P_{a,1}), \tag{55}$$

$$\sigma_\theta^{\mathrm{i}} = -\frac{\dfrac{(R_{\mathrm{i}}+T_{\mathrm{i}}/2)^2}{R^2}+1}{\dfrac{(R_{\mathrm{i}}+T_{\mathrm{i}}/2)^2}{(R_{\mathrm{i}}-T_{\mathrm{i}})^2}-1}P_i - \frac{1+\dfrac{(R_{\mathrm{i}}-T_{\mathrm{i}}/2)^2}{R^2}}{1-\dfrac{(R_{\mathrm{i}}-T_{\mathrm{i}}/2)^2}{(R_{\mathrm{i}}+T_{\mathrm{i}}/2)^2}}(-P_{a,1}), \quad R\in[R_{\mathrm{i}}-T_{\mathrm{i}}/2, R_{\mathrm{i}}+T_{\mathrm{i}}/2] \tag{56}$$

and, for the outer facesheet, are

$$\sigma_R^{\mathrm{o}} = -\frac{\dfrac{(R_{\mathrm{o}}+T_{\mathrm{o}}/2)^2}{R^2}-1}{\dfrac{(R_{\mathrm{o}}+T_{\mathrm{o}}/2)^2}{(R_{\mathrm{o}}-T_{\mathrm{o}}/2)^2}-1}(-P_{b,1}),$$

$$\sigma_\theta^{\mathrm{o}} = -\frac{\dfrac{(R_{\mathrm{o}}+T_{\mathrm{o}}/2)^2}{R^2}+1}{\dfrac{(R_{\mathrm{o}}+T_{\mathrm{o}}/2)^2}{(R_{\mathrm{o}}-T_{\mathrm{o}}/2)^2}-1}(-P_{b,1}), \quad R\in[R_{\mathrm{o}}-T_{\mathrm{o}}/2, R_{\mathrm{o}}+T_{\mathrm{o}}/2], \tag{57}$$

where σ_R^λ and σ_θ^λ ($\lambda=\mathrm{i},\mathrm{o}$) are the radial and circumferential normal stresses. With circumferentially axisymmetric boundary conditions, the strain-displacement relations of the isotropic facesheets read as

$$\varepsilon_R^\lambda = \frac{\mathrm{d}u_R^\lambda(R)}{\mathrm{d}R}, \quad \varepsilon_\theta^\lambda = \frac{u_R^\lambda(R)}{R}, \quad \gamma_{R\theta}^\lambda = 0, \quad R\in[R_\lambda - T_\lambda/2, R_\lambda + T_\lambda/2], \ \lambda=\mathrm{o},\mathrm{i}, \tag{58}$$

where u_R^λ are the radial displacements of the facesheets. As the core and facesheets are fully bonded along their mutual interfaces, the following compatibility conditions exist at the interfaces

$$u_R^{\mathrm{i}}\left(R_{\mathrm{i}}+\frac{T_{\mathrm{i}}}{2}\right) = u_R^{\mathrm{c}}\left(R_{\mathrm{i}}+\frac{T_{\mathrm{i}}}{2}\right), \quad u_R^{\mathrm{o}}\left(R_{\mathrm{o}}-\frac{T_{\mathrm{o}}}{2}\right) = u_R^{\mathrm{c}}\left(R_{\mathrm{o}}-\frac{T_{\mathrm{o}}}{2}\right). \tag{59}$$

From the constitutive equations of isotropic facesheets, we have

$$u_R^{\mathrm{i}}(R) = \frac{1}{E}[\sigma_\theta^{\mathrm{i}} - v(\sigma_Z^{\mathrm{i}} + \sigma_R^{\mathrm{i}})]R, \quad R\in[R_{\mathrm{i}}-T_{\mathrm{i}}/2, R_{\mathrm{i}}+T_{\mathrm{i}}/2], \tag{60}$$

$$u_R^{\mathrm{o}}(R) = \frac{1}{E}[\sigma_\theta^{\mathrm{o}} - v(\sigma_Z^{\mathrm{o}} + \sigma_R^{\mathrm{o}})]R, \quad R\in[R_{\mathrm{o}}-T_{\mathrm{o}}/2, R_{\mathrm{o}}+T_{\mathrm{o}}/2], \tag{61}$$

where E and v are the Young's modulus and Poisson ratio of the base material for the facesheets.

As shown in Figs. 5(c) and (d), equilibrium dictates that, for single-layered square cell

$$N_{x1} = 2P_{b,1}pR_{\mathrm{o}}/R_{\mathrm{i}} = 2P_{a,1}p \tag{62}$$

Please cite this article as: Liu, T., et al., Bi-functional optimization of actively cooled, pressurized hollow sandwich cylinders with prismatic..., J. Mech. Phys. Solids (2007), doi:10.1016/j.jmps.2007.04.007

and, for single-layered triangular cell:

$$N_{x2} = \frac{P_{b,1} p R_o}{R_i \sin(\phi)} = \frac{P_{a,1} p}{\sin(\phi)}, \tag{63}$$

where $p = w/2, \phi$ stands for the inclined angle for inclined core members (Figs. 4 and 5). Furthermore, from (59), we have

$$\frac{N_{x1}}{E/(1-v^2)T_{c1}} = \frac{\left[u_R^i\left(R_i + \frac{T_i}{2}\right) - u_R^o\left(R_o - \frac{T_o}{2}\right)\right]}{(T_c - T_o/2 - T_i/2)} \tag{64}$$

for single-layered square cell, and

$$\frac{N_{x2}}{E/(1-v^2)T_{c1}} = \frac{\left[u_R^i\left(R_i + \frac{T_i}{2}\right) - u_R^o\left(R_o - \frac{T_o}{2}\right)\right]}{(T_c - T_o/2 - T_i/2)} \tag{65}$$

for single-layered triangular cell. With Eqs. (59)–(65), $P_{a,1}, P_{b,1}$ can be readily solved. In these equations, the span p of the unit cell is assumed to be sufficiently small relative to the cylinder length L so that the bending deformation of facesheets within the span can be ignored.

Solutions for multilayered sandwich cylinders (Fig. 2) can be found in a way similar to that presented above for single-layered sandwich cylinders (see Liu et al., 2006). For these multilayered sandwich cylinders, the stresses in the core can be written as (see Fig. 5e):

$$\sigma_{R,j}^f = -\frac{\frac{(R_{f,j} + T_{fj}/2)^2}{R^2} - 1}{\frac{(R_{f,j} + T_{fj}/2)^2}{(R_{f,j} - T_{fj}/2)^2} - 1}(-P_{b,j}) - \frac{1 - \frac{(R_{f,j} - T_{fj}/2)^2}{R^2}}{1 - \frac{(R_{f,j} - T_{fj}/2)^2}{(R_{f,j} + T_{fj}/2)^2}}(-P_{a,j+1}), \tag{66}$$

$$\sigma_{\theta,j}^f = -\frac{\frac{(R_{f,j} + T_{fj}/2)^2}{R^2} + 1}{\frac{(R_{f,j} + T_{fj}/2)^2}{(R_{f,j} - T_{fj}/2)^2} - 1}(-P_{b,j}) - \frac{1 + \frac{(R_{f,j} - T_{fj}/2)^2}{R^2}}{1 - \frac{(R_{f,j} - T_{fj}/2)^2}{(R_{f,j} + T_{fj}/2)^2}}(-P_{a,j+1}),$$

$$R \in [R_{f,j} - T_{fj}/2, R_{f,j} + T_{fj}/2], \quad (j = 1, \ldots, n-1) \tag{67}$$

$$\sigma_{x,j}^c = \frac{2pP_{b,j}R_{f,j}}{R_i T_{cj}}, \quad \sigma_{z,j}^c = \frac{2pP_{b,j}R_{f,j}v}{R_i T_{cj}} \quad \text{(Square cell)}, \tag{68}$$

$$\sigma_{x,j}^c = \frac{pP_{b,j}R_{f,j}}{R_i T_{cj}\sin(\phi)}, \quad \sigma_{z,j}^c = \frac{pP_{b,j}R_{f,j}v}{R_i T_{cj}\sin(\phi)} \quad \text{(Triangular cell)}, \tag{69}$$

where $(\sigma_{R,j}^f, \sigma_{\theta,j}^f)$ are the stress components of the circumferential core member in the jth layer (Fig. 5e), $(\sigma_{x,j}^c, \sigma_{z,j}^c)$ are the normal stresses in the x and z-directions for the vertical and inclined core members in the jth layer (Fig. 5d), $(P_{b,j}, P_{a,j+1})$ are the interfacial stresses in the jth layer (Fig. 5e), and $R_{f,j}$ is the radius of the centroidal surface of the circumferential core member in the jth layer (Fig. 5e).

Please cite this article as: Liu, T., et al., Bi-functional optimization of actively cooled, pressurized hollow sandwich cylinders with prismatic..., J. Mech. Phys. Solids (2007), doi:10.1016/j.jmps.2007.04.007

4.2. The minimum mass design model

To seek the minimum mass design of a hollow sandwich-walled cylinder subjected to internal pressure, three failure modes are taken as the optimization constraints: facesheet yielding, core member yielding and core member buckling, given by

$$\frac{\sqrt{2}}{2}\left\{\left(\frac{\sigma_\theta^\lambda}{E}-\frac{\sigma_R^\lambda}{E}\right)^2+\left(\frac{\sigma_Z^\lambda}{E}-\frac{\sigma_R^\lambda}{E}\right)^2+\left(\frac{\sigma_Z^\lambda}{E}-\frac{\sigma_\theta^\lambda}{E}\right)^2\right\}^{1/2}\leqslant\sigma_Y/E$$

$$(\lambda=\mathrm{i},\mathrm{o})\quad\text{(Facesheet yielding)},\tag{70}$$

$$\frac{\sqrt{2}}{2}\left\{\left(\frac{\sigma_{\theta,j}^f}{E}-\frac{\sigma_{R,j}^f}{E}\right)^2+\left(\frac{\sigma_{Z,j}^f}{E}-\frac{\sigma_{R,j}^f}{E}\right)^2+\left(\frac{\sigma_{Z,j}^\lambda}{E}-\frac{\sigma_{\theta,j}^f}{E}\right)^2\right\}^{1/2}\leqslant\sigma_Y/E$$

(Circumferential core member yielding for the jth layer), (71)

$$\frac{\sqrt{2}}{2}\left\{\left(\frac{\sigma_{x,j}^c}{E}-\frac{\sigma_{z,j}^c}{E}\right)^2+\left(\frac{\sigma_{x,j}^c}{E}\right)^2+\left(\frac{\sigma_{z,j}^c}{E}\right)^2\right\}^{1/2}\leqslant\frac{\sigma_Y}{E}$$

(Vertical or inclined core member yielding for the jth layer), (72)

$$\frac{\sigma_{x,j}^c}{E}\leqslant\frac{\kappa\pi^2(T_{cj}/R_\mathrm{o})^2\sin^2\phi}{12(1-v^2)(l_j/R_\mathrm{o})^2}$$

(Vertical or inclined core member buckling for the jth layer), (73)

where, in (73), both the vertical and inclined core members are assumed to be simply supported, with the buckling coefficient $\kappa=1$ (see Liu et al., 2006), and l_j is the length of the vertical or inclined core member in the jth layer (Fig. 4). Subjected to the constraints of (68)–(71), the minimization of structural mass can be written as

Model II:

$$\begin{aligned}\text{Min }\chi_2(\boldsymbol{\Lambda})&=\frac{W}{R_\mathrm{o}^2}\\&=\rho_\mathrm{s}\pi\left\{(1-\xi)\left[\left(1-\frac{1}{2}\frac{T_\mathrm{o}}{R_\mathrm{o}}\right)^2-\left(\frac{R_\mathrm{i}}{R_\mathrm{o}}+\frac{1}{2}\frac{T_\mathrm{i}}{R_\mathrm{o}}\right)^2\right]+2\frac{T_\mathrm{o}}{R_\mathrm{o}}+2\frac{R_\mathrm{i}}{R_\mathrm{o}}\frac{T_\mathrm{i}}{R_\mathrm{o}}\right\},\end{aligned}\tag{74}$$

where W denotes the structural mass per unit length. The geometrical design variables are defined in Section 2.2 and Eqs. (52) and (53).

Based on the above minimum mass design model, sandwich cylinders with either square- or triangular-celled core are optimized. Throughout the paper, the optimization problem is solved using the Multi-island Genetic Algorithm optimizer embedded in a commercially available optimization solution engine iSIGHT^{TM}, with the main programs coded in Matlab^{TM}. The material is assumed to be representative of a structural steel, with $\sigma_Y/E=0.001$, $v=0.3$, $\rho_\mathrm{s}=7900\,\mathrm{kg/m^3}$, $k_\mathrm{s}=60.5\,\mathrm{W/(mK)}$. The outer radius, R_o, of the cylinder is assumed to vary in a way such that additional geometrical constraints of $T_J/R_\mathrm{o}\geqslant0.001$ ($J=\mathrm{i},\mathrm{c},\mathrm{o}$) and $0.9\geqslant R_\mathrm{i}/R_\mathrm{o}\geqslant0.5$ are satisfied. The former is based on the consideration of manufacturing possibilities, whilst the latter aims to make the shell of the

Please cite this article as: Liu, T., et al., Bi-functional optimization of actively cooled, pressurized hollow sandwich cylinders with prismatic..., J. Mech. Phys. Solids (2007), doi:10.1016/j.jmps.2007.04.007

sandwich cylinders relatively thin due to size constraint in practice (for example, the cylindrical combustor in an engine is normally integrated with another structure, Raskie, 2006). The lower bound and upper bound of channel number per layer, $\widetilde{N}$, is set to 10 and 40, respectively, for a channel number within these bounds is acceptable for both the small p assumption (see Section 4.1) and fabrication considerations. The load parameter P_i/E is assumed to vary within $10^{-5}\sim15\times10^{-5}$, which covers the practical case of a steel combustor with $P_i = 10\,\text{MPa}$ (Raskie, 2006). The maximum layer number for both kinds of core topologies is $j_{\max} = 8$, as more layers would cause complexities in fabrication.

The outcome of the minimum mass optimization is plotted in Figs. 6(a) and (b) for the square- and triangular-celled core sandwich cylinder, respectively. The results of Fig. 6 clearly demonstrate the significant structural advantage of both types of sandwich cylinder over a solid-walled hollow cylinder. The structural performance of the square-celled core sandwich is slightly better than that with triangular-celled core, and is not sensitive to the number of core layers (Fig. 6a), because the thickness (or length of radial core members) of each sandwich layer can vary according to the stress gradient. The minimum mass of a triangular-celled core sandwich is more sensitive to the number of core layer, with the optimal layer number $j_{\text{opt}} = 4$ (Fig. 6b), for each sandwich layer must maintain a uniform thickness during optimization. For both core topologies, the failure modes are simultaneous inner facesheet yielding and core member buckling, and the minimum mass always occurs when $\widetilde{N} = 10, R_i/R_o = 0.5$ for a square-celled core sandwich cylinder and $\widetilde{N} = 10\sim30$, $R_i/R_o = 0.5$ for a triangular-celled core sandwich cylinder.

To understand further why an internally pressurized hollow sandwich cylinder structurally outperforms its equivalent solid-walled cylinder, analytical solutions for the minimum masses of a single layer square-celled core sandwich cylinder and a solid-walled cylinder are presented for comparison in Appendix.

5. Bi-objective optimizations

5.1. Design model for optimal thermo-mechanical performance

Based on Sections 3 and 4, further optimization can be performed on hollow sandwich cylinders with two different objectives simultaneously: one is for optimal structural weight efficiency, e.g., the minimum mass design, whilst the other is for optimal heat transfer performance of the cellular core, e.g., the maximum $(Q_I/L)/R_o^{1/2}(t_w - t_{f,in})$ design. Unlike single objective optimizations, in most cases, the two objectives may compete with each other in optimization, so that the solution to the bi-objective problem is not a single point, but a family of points (the Pareto-optimal set). Here, each point is regarded as optimum in the sense that any improvement in one objective can only take place if the other objective worsens. However, since the Pareto-optimal set is not single-valued, it is difficult to use the data set to compare and assess the thermo-mechanical performances of hollow sandwich cylinders with different core topologies. In view of this, by combining the two objectives in a single equation, a non-dimensional index, Ξ, can be alternatively formulated, which is defined as

$$\Xi = \frac{Q/L}{W/R_o^2 v_f c_p (t_w - t_{f,in})}. \tag{75}$$

In Eq. (75), Ξ is normalized by v_f and c_p, which also represent the thermal properties of a

Please cite this article as: Liu, T., et al., Bi-functional optimization of actively cooled, pressurized hollow sandwich cylinders with prismatic..., J. Mech. Phys. Solids (2007), doi:10.1016/j.jmps.2007.04.007

coolant, as shown in Eqs. (50) and (51). Here, ρ_f is relevant to v_f and c_p; generally, the bigger ρ_f is the smaller v_f and c_p are. Hence, the physical implication of Ξ can be understood as the heat transfer rate per unit length carried by unit structural mass with a

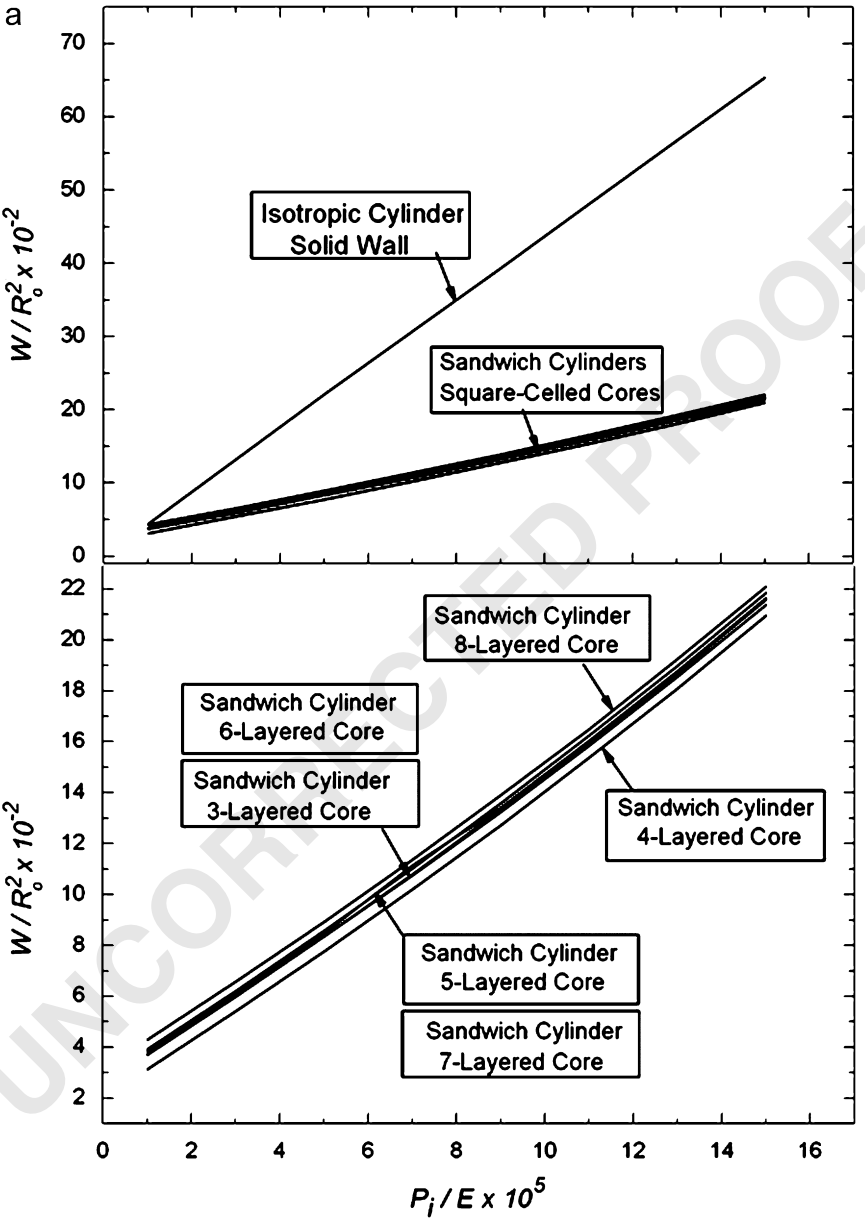

Fig. 6. W/R_o^2 plotted as function of dimensionless load parameter for hollow sandwich cylinders with (a) square cells and (b) triangular cells, all calculated with $\rho_s = 7900\,\mathrm{kg/m^3}$, $\sigma_Y/E = 0.001$, $v = 0.3$, $\kappa = 1$, $T_J/R_o \geqslant 0.001$ ($J = \mathrm{i, c, o}$) and $0.9 \geqslant R_i/R_o \geqslant 0.5$.

Please cite this article as: Liu, T., et al., Bi-functional optimization of actively cooled, pressurized hollow sandwich cylinders with prismatic..., J. Mech. Phys. Solids (2007), doi:10.1016/j.jmps.2007.04.007

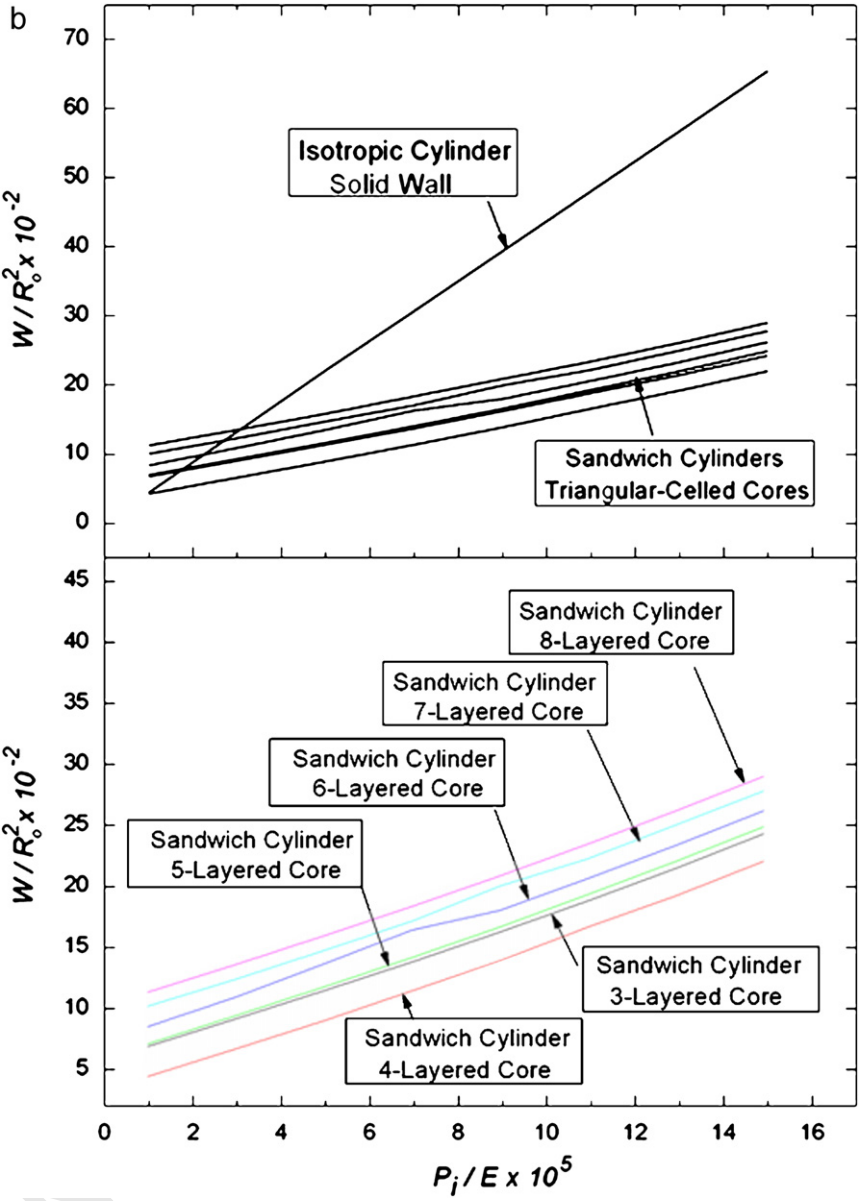

Fig. 6. (*Continued*)

given coolant and a prescribed temperature boundary: the greater is the value of Ξ, the better is the efficiency of the bi-functionality. Hence, with (46)–(49) and (70)–(73) acting as the constraints, the thermo-mechanical optimization model can be described as:

Please cite this article as: Liu, T., et al., Bi-functional optimization of actively cooled, pressurized hollow sandwich cylinders with prismatic..., J. Mech. Phys. Solids (2007), doi:10.1016/j.jmps.2007.04.007

Model III:

$$\text{Max}\,\chi_3(\mathbf{\Lambda}) = \frac{\Xi}{R_o^{1/2}} = \frac{(P\widetilde{N})^{1/2}\rho_f^{1/2}}{\pi v_f^{3/2}\rho_s} \frac{\dfrac{1}{\left(\dfrac{L}{R_o}\right)^{3/2}}\sqrt{\displaystyle\sum_{j=1}^{n}\left(\frac{\left(\dfrac{D_{h,aj}}{R_o}\right)^2\left(\dfrac{A_{aj}}{R_o^2}\right)}{32\Psi_{aj}}\right)}}{\left\{(1-\xi)\left[\left(1-\dfrac{1T_o}{2R_o}\right)^2-\left(\dfrac{R_i}{R_o}+\dfrac{1T_i}{2R_o}\right)^2\right]+2\dfrac{T_o}{R_o}+2\dfrac{R_i\,T_i}{R_o R_o}\right\}}$$

(Square-celled core sandwich cylinder), (76)

$$\text{Max}\,\chi_3(\mathbf{\Lambda}) = \frac{\Xi}{R_o^{1/2}} = \frac{(P\widetilde{N})^{1/2}\rho_f^{1/2}}{\pi v_f^{3/2}\rho_s} \frac{\dfrac{1}{\left(\dfrac{L}{R_o}\right)^{3/2}}\sqrt{\displaystyle\sum_{j=1}^{n}\left(\frac{\left(\dfrac{D_{h,cj}}{R_o}\right)^2\left(\dfrac{A_{cj}}{R_o^2}\right)}{32\Psi_{cj}}+\frac{\left(\dfrac{D_{h,tj}}{R_o}\right)^2\left(\dfrac{A_{tj}}{R_o^2}\right)}{32\Psi_{tj}}\right)}}{\left\{(1-\xi)\left[\left(1-\dfrac{1T_o}{2R_o}\right)^2-\left(\dfrac{R_i}{R_o}+\dfrac{1T_i}{2R_o}\right)^2\right]+2\dfrac{T_o}{R_o}+2\dfrac{R_i\,T_i}{R_o R_o}\right\}}$$

(Triangular-celled core sandwich cylinder). (77)

Here, again, the geometrical design variables are defined in Section 2.2 and Eqs. (52) and (53).

In the sections to follow, we first compare the three design models described in Eqs. (50), (51), (74), (76) and (77) for a three-layered core sandwich cylinder having square cells, then present the results for the thermo-mechanically optimized hollow sandwich cylinders with different core topologies.

5.2. Comparisons of different optimization models

Square-celled core sandwich cylinders are optimized in this section to compare the three optimization models: the maximum $(Q_I/L)/R_o^{1/2}(t_w - t_{f,in})$ design model, the minimum W/R_o^2 design model and the maximum $\Xi/R_o^{1/2}$ design model, which are separately described in Sections 3–5. For simplicity, the number of core layers is fixed at three. The results presented below are calculated with $\widehat{P} = 0.5\,\text{W}$, $L = 2R_o$, $k_s = \text{inf}$, $R_o = 0.12\,\text{m}$, and $\xi \geqslant 0.8$, with air acting as the working coolant. The geometrical design variables are defined in Section 2.2 and Eqs. (52) and (53).

The outcome of the minimum W/R_o^2 design and the maximum $\Xi/R_o^{1/2}$ design is shown in Figs. 7 and 8, with Figs. 7(a) and 8(a) presenting the results for selected values of the dimensionless load parameter P_i/E and Figs. 7(b) and 8(b) plotting the optimization results against P_i/E. The four loading parameters in Figs. 7(a) and 8(a) represent lightly, moderately (with two loading parameters) and heavily loaded cases, respectively, and the corresponding results are plotted as functions of the number of channels per layer $\widetilde{N}$ to

Please cite this article as: Liu, T., et al., Bi-functional optimization of actively cooled, pressurized hollow sandwich cylinders with prismatic..., J. Mech. Phys. Solids (2007), doi:10.1016/j.jmps.2007.04.007

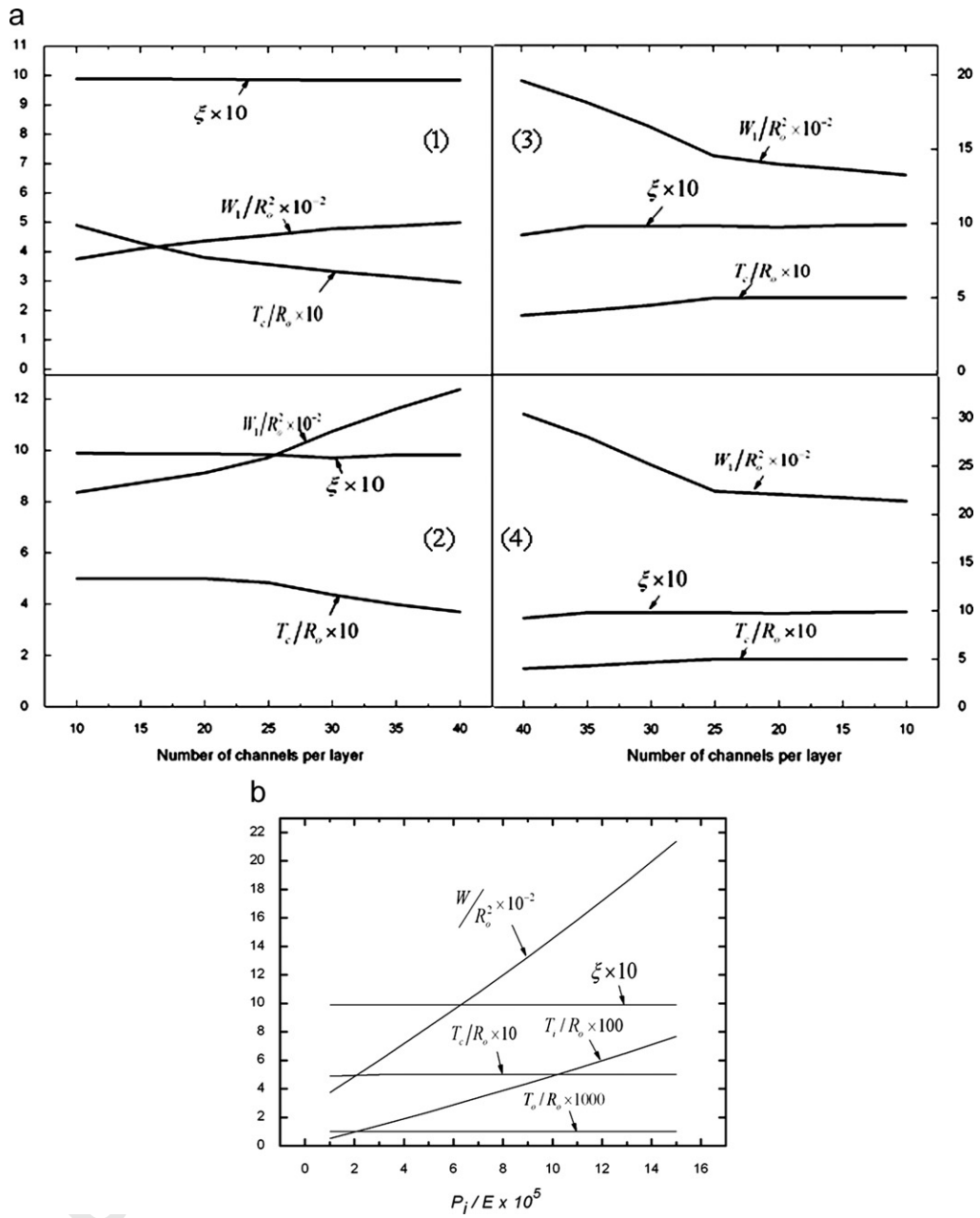

Fig. 7. Geometric parameters and values of W/R_o^2 of optimally designed three-layered sandwich cylinders having square cells plotted as functions of: (a) number of channels per layer and (b) dimensionless load parameter, all calculated with $\kappa = 1$, $\sigma_Y/E = 0.001$, $v = 0.3$, $\rho_s = 7900\,\mathrm{kg/m^3}$, $0.9 \geqslant R_i/R_o \geqslant 0.5$, $T_J/R_o \geqslant 0.001$ ($J = i, c, o$) and based on maximum W/R_o^2 design model. The four loading parameters considered in (a) are (1) $P_i/E = 10^{-5}$, (2) $P_i/E = 5\times10^{-5}$, (3) $P_i/E = 9\times10^{-5}$ and (4) $P_i/E = 15\times10^{-5}$. All the optimal designs in (b) occur at $\widetilde{N} = 10$ and $R_i/R_o = 0.5$.

Please cite this article as: Liu, T., et al., Bi-functional optimization of actively cooled, pressurized hollow sandwich cylinders with prismatic..., J. Mech. Phys. Solids (2007), doi:10.1016/j.jmps.2007.04.007

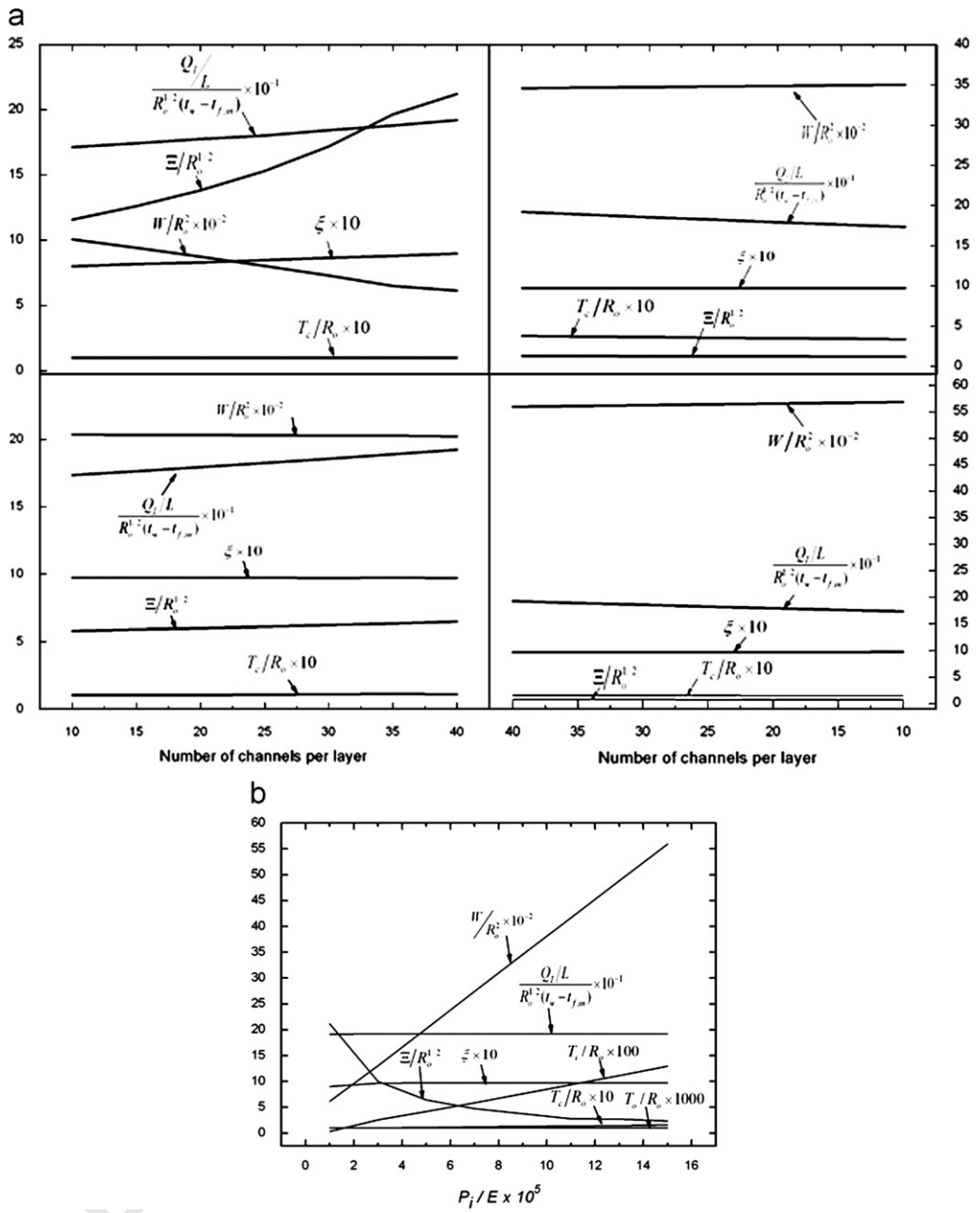

Fig. 8. Geometric parameters and values of W/R_o^2, $\Xi/R_o^{1/2}$ and $(Q_1/L)/R_o^{1/2}(t_w - t_{f,in})$ of optimally designed three-layered sandwich cylinders with square cells plotted as functions of: (a) number of channels per layer and (b) dimensionless load parameter, all calculated with $R_o = 0.12\,m$, $k_s = inf$, $\kappa = 1$, $\rho_s = 7900\,kg/m^3$, $\xi \geqslant 0.8$, $L = 2R_o$, $\widehat{P} = 0.5\,W$, $\sigma_Y/E = 0.001$, $v = 0.3$, $T_J/R_o \geqslant 0.001$ $(J = i, c, o)$, $0.9 \geqslant R_i/R_o \geqslant 0.5$ and based on maximum $\Xi/R_o^{1/2}$ design model; the working coolant is air. The four loading parameters considered in (a) are: (1) $P_i/E = 10^{-5}$, (2) $P_i/E = 5\times 10^{-5}$, (3) $P_i/E = 9\times 10^{-5}$ and (4) $P_i/E = 15\times 10^{-5}$. All the optimal designs in (b) occur at $\widetilde{N} = 40$ and $R_i/R_o \approx 0.1$.

Please cite this article as: Liu, T., et al., Bi-functional optimization of actively cooled, pressurized hollow sandwich cylinders with prismatic..., J. Mech. Phys. Solids (2007), doi:10.1016/j.jmps.2007.04.007

explore its influence upon optimization. In the next section, $\widetilde{N}$ itself will be treated as a design variable, so that it can be optimized.

With the minimum structural mass design model (Fig. 7), the minimum value of W/R_o^2 increases with $\widetilde{N}$, whilst T_c/R_o decreases as $\widetilde{N}$ is increased. Therefore, all the optimal designs occur at $\widetilde{N}=10$ and $R_i/R_o=0.5$. For the maximum $\Xi/R_o^{1/2}$ design model, the value of $\Xi/R_o^{1/2}$ increases with $\widetilde{N}$ while the value of T_c/R_o stays unchanged over the range of $\widetilde{N}$ considered (Fig. 8a). The maximum of $\Xi/R_o^{1/2}$ always happens at $\widetilde{N}=40$ and $R_i/R_o\approx 0.1$. The two different variation trends show the two objectives (thermal and structural) coupled by the index Ξ compete with each other during optimization. For both models, as shown in Figs. 7(b) and 8(b), the geometry of the core has almost no change as P_i is changed, since the variation of ξ and T_c/R_o with respect to P_i is negligible. The values of both W/R_o^2 and T_i/R_o increase linearly against P_i, whilst that of T_o/R_o is always fixed at the lower bound (0.001). Therefore, it could be deduced that the mass increase of the sandwich cylinder with increasing P_i is mainly caused by the thickness increase of the inner facesheet, T_i. For all the loading cases, the governing failure modes are simultaneous inner facesheet yielding and core member buckling for the minimum W/R_o^2 model, and inner facesheet yielding alone for the maximum $\Xi/R_o^{1/2}$ model.

Figs. 9(a) and (b) plot separately the results of the maximum $(Q_I/L)/R_o^{1/2}(t_w-t_{f,in})$ design model and the maximum $\Xi/R_o^{1/2}$ design model, both *without mechanical loading* ($P_i=0$). It is observed that whilst the values of T_c/R_o, ξ and $(Q_I/L)/R_o^{1/2}(t_w-t_{f,in})$ obtained by the two optimization models are very close, W/R_o^2 has a much smaller value for the maximum $\Xi/R_o^{1/2}$ design model. As mentioned in Section 3.3, the solution for *model* I may not be unique. Hence, the results of Fig. 9 derived from both design models are all solutions for *model* I. It is obvious, in this case, that the result of the maximum $\Xi/R_o^{1/2}$ design is the one with the lightest weight amongst all the results corresponding to the maximum $(Q_I/L)/R_o^{1/2}(t_w-t_{f,in})$ design. Upon comparing Fig. 9 (*without mechanical loading*) with Fig. 8(b) (*with mechanical loading*), it is interesting to observe that the values of T_c/R_o, ξ and $(Q_I/L)/R_o^{1/2}(t_w-t_{f,in})$ are also very close for the two different scenarios, suggesting that the core geometry has little change among these cases, whilst the results plotted in Fig. 8(b) represent the solution for *model* I with heavier structural mass to support the mechanical load.

According to the analysis presented above, for the optimized designs based on the maximum $\Xi/R_o^{1/2}$ design model, the sandwich core tends to maintain the geometry for maximum heat transfer performance, whilst the sizes of facesheets vary against mechanical load to reduce the structural mass. Therefore, the index Ξ acts well in the assessment of the combinational performance of sandwich cylinders. Consequently, in the following sections, the maximum $\Xi/R_o^{1/2}$ design model will be employed to evaluate the bi-functional performance of hollow sandwich cylinders.

6. Optimal thermo-mechanical performance of 2D cellular-cored sandwich cylinder

In this section, square- and triangular-celled core sandwich cylinders are optimized to compare their thermo-mechanical performances and understand the influences of geometric parameters of the structure. The hollow cylinder is pressurized internally by P_i, with its inner surface kept isothermally at temperature t_w. The geometrical design variables are defined in Section 2.2 and Eqs. (52) and (53). The number of channels per layer $\widetilde{N}$ is treated as a design variable, so that it can be optimized.

Please cite this article as: Liu, T., et al., Bi-functional optimization of actively cooled, pressurized hollow sandwich cylinders with prismatic..., J. Mech. Phys. Solids (2007), doi:10.1016/j.jmps.2007.04.007

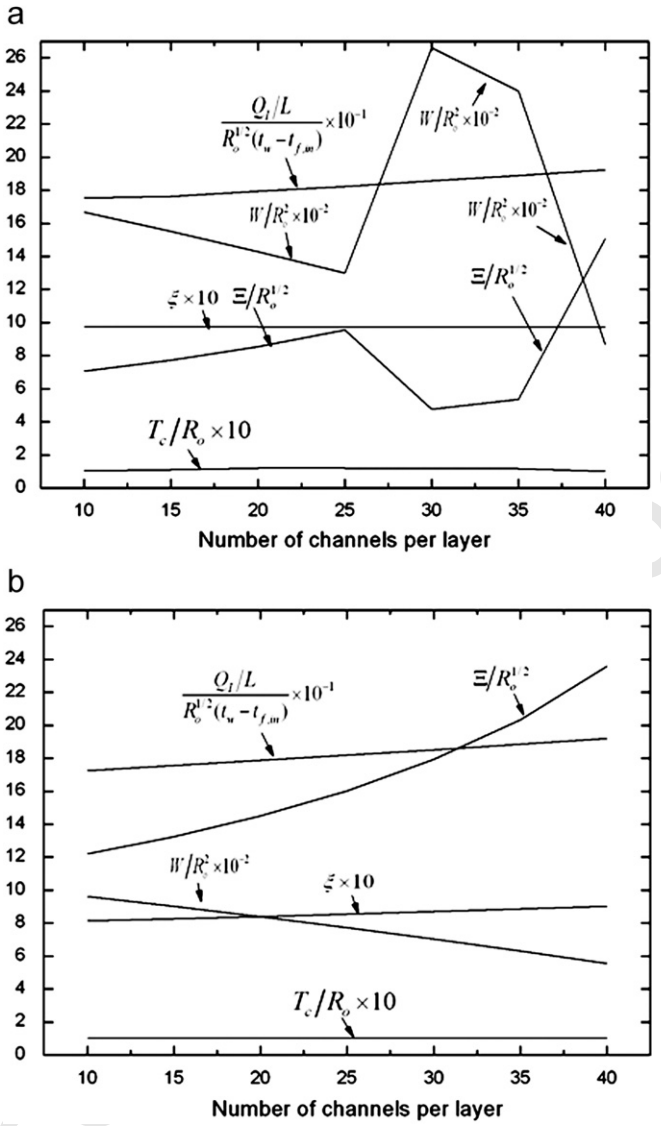

Fig. 9. Geometric parameters and values of W/R_o^2, $\Xi/R_o^{1/2}$ and $(Q_I/L)/R_o^{1/2}(t_w - t_{f,in})$ of optimally designed three-layered hollow sandwich cylinders having square cells plotted as functions of number of channels per layer, all calculated with $\rho_s = 7900\,kg/m^3$, $k_s = inf$, $R_o = 0.12\,m$, $\xi \geqslant 0.8$, $\widehat{P} = 0.5\,W$, $L = 2R_o$, $0.9 \geqslant R_i/R_o \geqslant 0.5$, $T_J/R_o \geqslant 0.001$ ($J = i, c, o$) and *without mechanical loading*; the working coolant is air. The design models are: (a) maximum $(Q_I/L)/R_o^{1/2}(t_w - t_{f,in})$ model and (b) maximum $\Xi/R_o^{1/2}$ model.

The outcome of the optimized square-celled core sandwiches, with selected global lengths $L = 2R_o$, $L = 5R_o$ and $L = 10R_o$, is plotted in Figs. 10–12 for $\Xi/R_o^{1/2}$, W/R_o^2 and $(Q_I/L)/R_o^{1/2}(t_w - t_{f,in})$, respectively, all based on the maximum $\Xi/R_o^{1/2}$ design model (Section 5). The parameters used for the calculation are $\widehat{P} = 0.5\,W$, $k_s = 60.5\,W/mK$ and $R_o = 0.12\,m$, and air is used as the coolant. Meanwhile, to maintain a low mass of the

Please cite this article as: Liu, T., et al., Bi-functional optimization of actively cooled, pressurized hollow sandwich cylinders with prismatic..., J. Mech. Phys. Solids (2007), doi:10.1016/j.jmps.2007.04.007

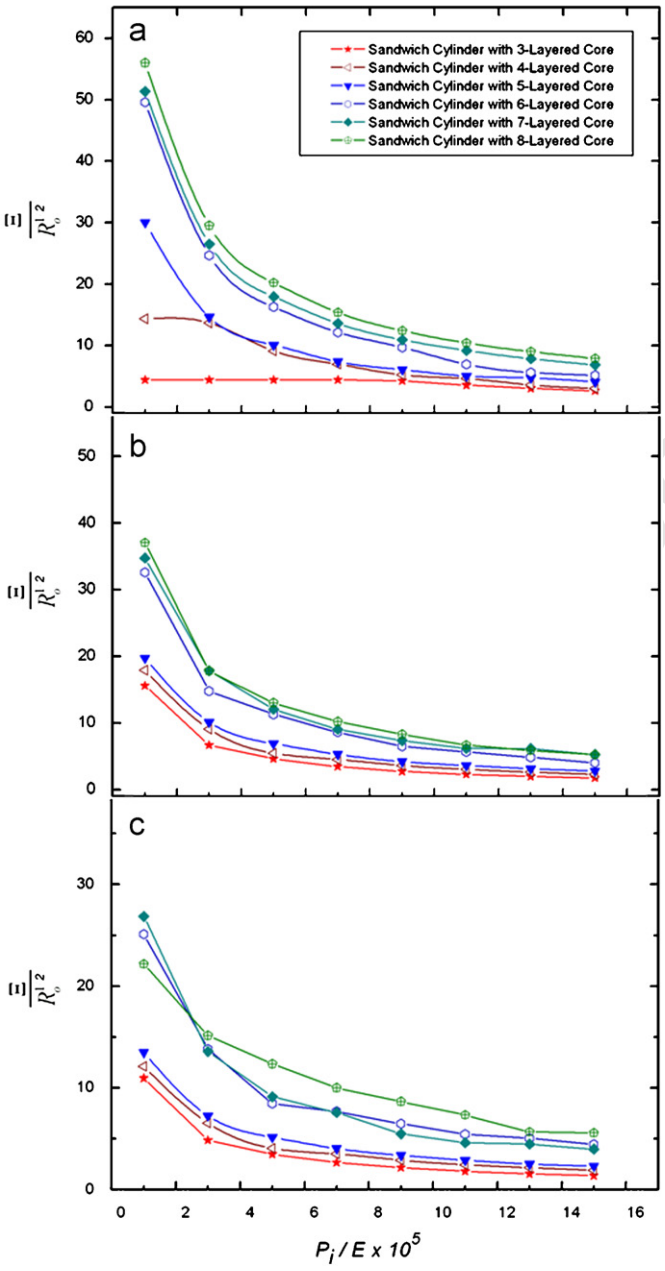

Fig. 10. $\Xi/R_o^{1/2}$ plotted as function of dimensionless load parameter for optimally designed sandwich cylinders with square cells and total length of: (a) $L = 2R_o$, (b) $L = 5R_o$ and (c) $L = 10R_o$, all calculated with $R_o = 0.12\,\mathrm{m}$, $\sigma_Y/E = 0.001$, $v = 0.3$, $k_s = 60.5\,\mathrm{W/mK}$, $\rho_s = 7900\,\mathrm{kg/m^3}$, $\xi \geqslant 0.8$, $\widehat{P} = 0.5\,\mathrm{W}$, $T_J/R_o \geqslant 0.001$ $(J = \mathrm{i}, \mathrm{c}, \mathrm{o})$, $0.9 \geqslant R_i/R_o \geqslant 0.5$ and based on *maximum* $\Xi/R_o^{1/2}$ *design model*; the working coolant is air.

Please cite this article as: Liu, T., et al., Bi-functional optimization of actively cooled, pressurized hollow sandwich cylinders with prismatic..., J. Mech. Phys. Solids (2007), doi:10.1016/j.jmps.2007.04.007

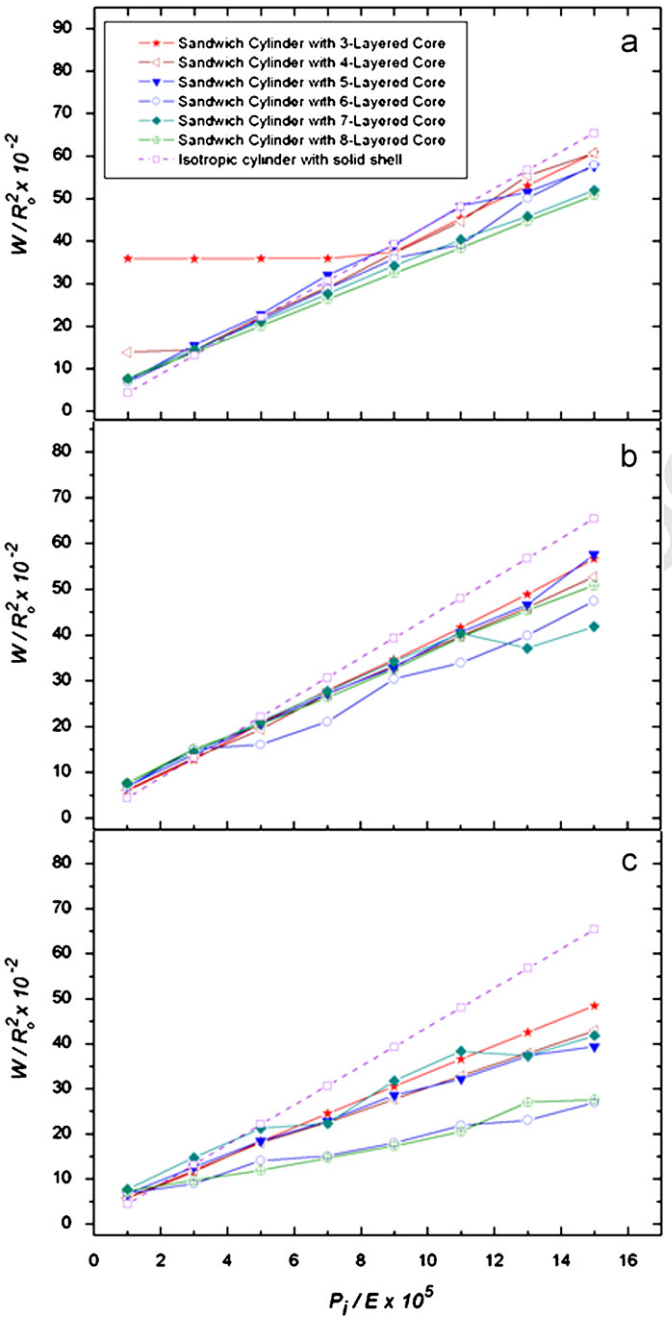

Fig. 11. W/R_o^2 plotted as function of dimensionless load parameter for optimally designed sandwich cylinders with square cells and total length of: (a) $L = 2R_o$, (b) $L = 5R_o$ and (c) $L = 10R_o$, all calculated with $R_o = 0.12\,\mathrm{m}$, $\sigma_Y/E = 0.001$, $v = 0.3$, $k_s = 60.5\,\mathrm{W/mK}$, $\rho_s = 7900\,\mathrm{kg/m^3}$, $\xi \geqslant 0.8$, $\widehat{P} = 0.5\,\mathrm{W}$, $T_J/R_o \geqslant 0.001$ ($J = \mathrm{i,c,o}$), $0.9 \geqslant R_i/R_o \geqslant 0.5$ and based on *maximum* $\Xi/R_o^{1/2}$ *design model*; the working coolant is air. The minimum weight of solid-walled hollow cylinder with same base material is plotted for comparison.

Please cite this article as: Liu, T., et al., Bi-functional optimization of actively cooled, pressurized hollow sandwich cylinders with prismatic..., J. Mech. Phys. Solids (2007), doi:10.1016/j.jmps.2007.04.007

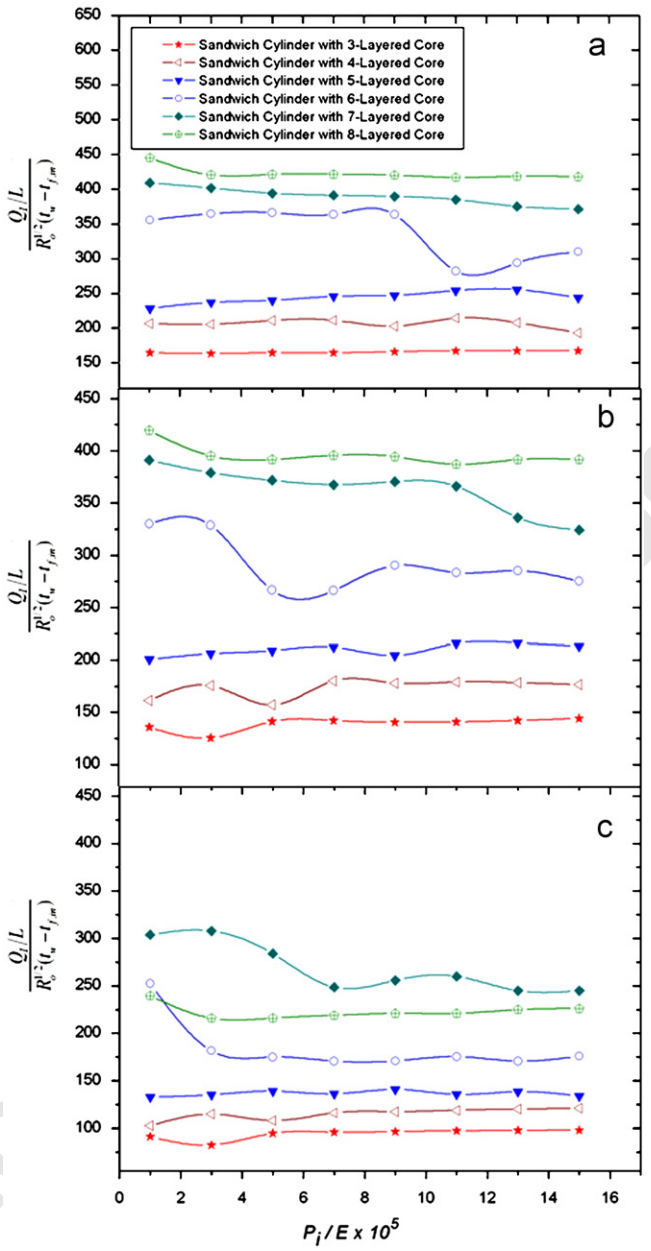

Fig. 12. $(Q_l/L)/R_o^{1/2}(t_w - t_{f,in})$ plotted as function of dimensionless load parameter for optimally designed sandwich cylinders with square cells and total length of: (a) $L = 2R_o$, (b) $L = 5R_o$ and (c) $L = 10R_o$, all calculated with $R_o = 0.12\,\mathrm{m}$, $\sigma_Y/E = 0.001$, $v = 0.3$, $k_s = 60.5\,\mathrm{W/mK}$, $\rho_s = 7900\,\mathrm{kg/m^3}$, $\xi \geqslant 0.8$, $\widehat{P} = 0.5\,\mathrm{W}$, $T_J/R_o \geqslant 0.001$ $(J = \mathrm{i,c,o})$, $0.9 \geqslant R_i/R_o \geqslant 0.5$ and based on *maximum* $\Xi/R_o^{1/2}$ *design model*; the working coolant is air.

Please cite this article as: Liu, T., et al., Bi-functional optimization of actively cooled, pressurized hollow sandwich cylinders with prismatic..., J. Mech. Phys. Solids (2007), doi:10.1016/j.jmps.2007.04.007

cellular core, a lower bound of 0.8 is set for its porosity ξ. The effects of both R_o (external radius of cylinder) and coolant will be discussed later. As mentioned by Wen et al. (2007), for the thermal optimization of flat panels, the optimal porosity ξ does not rely on $\widehat{P}$ (pumping power). Hence, it can be deduced that $\widehat{P}$ is not the dominant factor to influence the final optimization results for curved panels, as in this paper.

As shown in Fig. 10, the maximum of $\Xi/R_o^{1/2}$ occurs mainly at eight-layered square-celled core sandwiches for the three cylinder lengths selected and all loading parameters concerned. The cylinder length has a significant influence on the value of $\Xi/R_o^{1/2}$. Generally, the shorter is the cylinder, the greater is the value of $\Xi/R_o^{1/2}$ (with the exception of lightly loaded three and four layered core sandwiches). When the thermo-mechanical performances of sandwiches with different core topology layers are close, the one with the least number of layers may be regarded as the optimal design for ease of fabrication. For example, the thermo-mechanical performances of six–eight layered sandwiches are close for relatively short cylinder lengths ($L \leqslant 5R_o$), so that the six-layered sandwich may be regarded as the optimal design in such cases. It is striking to find, although W/R_o^2 for the maximum $\Xi/R_o^{1/2}$ designs have values (Fig. 11) greater than those of the minimum mass designs (Fig. 6a), they are equivalent to or less than the minimum mass of a solid-walled hollow cylinder (with the exception of lightly loaded three and four layered sandwiches with relatively short length L). Similar to the optimal three-layered sandwich cylinder of Section 5.1, the failure mode is inner facesheet yielding (with the exception of lightly loaded three and four layered core sandwiches) and the optimum always occurs at the upper bound $\widetilde{N} = 40$. Compare the results of the two three-layered core sandwiches with only difference of k_s, as separately shown in Fig. 8(b) ($k_s = \text{inf}$) and Figs. 10–12(a) ($k_s = 60.5\,\text{W/mK}$), masses of one with greater thermal resistance ($k_s = 60.5\,\text{W/mK}$) keep constant for the lightly loaded cases, and without occurrence of structural failure (also for lightly loaded four layered core sandwiches), which means the bi-functional optimization is mainly controlled by its thermal performance in such situations.

In most cases, as shown in Fig. 12, the variation of $(Q_I/L)/R_o^{1/2}(t_w - t_{f,in})$ (*model* II) with varying loading parameter for each individual core topology is not vigorous. Hence, combining Figs. 10–12, we find that a variation trend similar to that mentioned in Section 5.2 has been followed: the core geometry is optimized to achieve a good heat transfer performance, whilst the facesheets are optimized to support the internal pressure.

To understand the effect of coolant, Fig. 13 compares the values of $\Xi/R_o^{1/2}$ for optimally designed eight- and six-layered sandwich cylinders having square cells for selected global lengths $L = 5R_o$ and $L = 10R_o$ ($R_o = 0.12\,\text{m}$). The working coolant is water. As suggested by Fig. 13, the maximum of $\Xi/R_o^{1/2}$ still occurs at eight-layered square-celled core sandwiches for the two selected global lengths, and the shorter is the cylinder, the greater is the value of $\Xi/R_o^{1/2}$. These trends are same to that when the working coolant is air, as mentioned above. Different from above (the working coolant is air), in such cases, the optimum always occurs at the lower bound $\widetilde{N} = 10$.

To understand the effect of R_o (external radius of cylinder), Fig. 14 compares the values of $\Xi/R_o^{1/2}$ for optimally designed eight-layered sandwich cylinders having square cells for selected values of R_o. Fig. 14 suggests that, although a smaller R_o leads to a greater $\Xi/R_o^{1/2}$, the increase is small. Hence, the results presented in Figs. 10–11 can represent the general trend of R_o.

For simplicity, the bi-functional optimal results of sandwich cylinders having triangular cells are not shown here. For this type of cylinder, it is found that four- and five-layered

Please cite this article as: Liu, T., et al., Bi-functional optimization of actively cooled, pressurized hollow sandwich cylinders with prismatic..., J. Mech. Phys. Solids (2007), doi:10.1016/j.jmps.2007.04.007

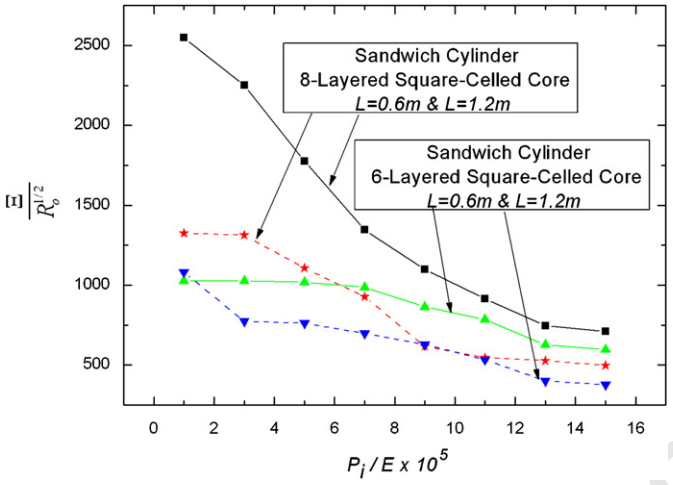

Fig. 13. $\Xi/R_o^{1/2}$ plotted as function of dimensionless load parameter for optimally designed eight- and six-layered sandwich cylinders with square cells and two global lengths $L = 0.6\,\mathrm{m}$ and $L = 1.2\,\mathrm{m}$, all calculated with $R_o = 0.12\,\mathrm{m}$, $\sigma_Y/E = 0.001$, $v = 0.3$, $k_s = 60.5\,\mathrm{W/mK}$, $\rho_s = 7900\,\mathrm{kg/m^3}$, $\xi \geqslant 0.8$, $\widehat{P} = 0.5\,\mathrm{W}$, $T_J/R_o \geqslant 0.001$ ($J = \mathrm{i,c,o}$), $0.9 \geqslant R_i/R_o \geqslant 0.5$ and based on *maximum* $\Xi/R_o^{1/2}$ *design model*; the working coolant is water. The solid line stands for the values of $L = 0.6\,\mathrm{m}$, the dashed line stands for the values of $L = 1.2\,\mathrm{m}$.

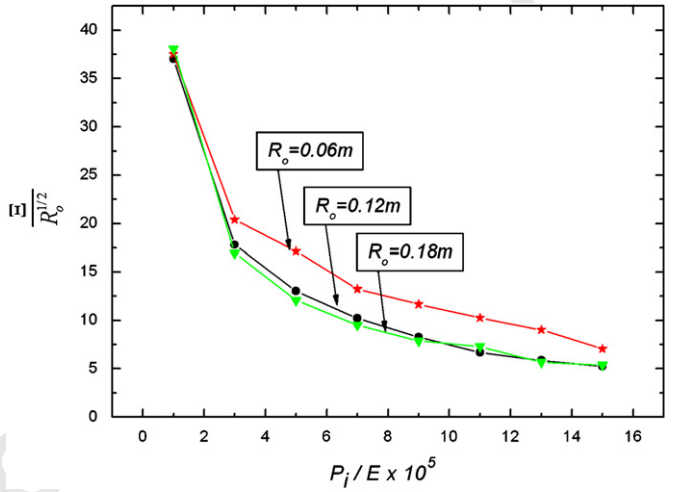

Fig. 14. $\Xi/R_o^{1/2}$ plotted as function of dimensionless load parameter for optimally designed eight-layered sandwich cylinders with square cells and three different values of R_o, all calculated with $L = 0.6\,\mathrm{m}$, $\sigma_Y/E = 0.001$, $v = 0.3$, $k_s = 60.5\,\mathrm{W/mK}$, $\rho_s = 7900\,\mathrm{kg/m^3}$, $\xi \geqslant 0.8$, $\widehat{P} = 0.5\,\mathrm{W}$, $T_J/R_o \geqslant 0.001$ ($J = \mathrm{i,c,o}$), $0.9 \geqslant R_i/R_o \geqslant 0.5$ and based on *maximum* $\Xi/R_o^{1/2}$ *design model*; the working coolant is air.

sandwiches have the best bi-functional performance amongst all core topologies concerned. The optimally designed eight- and six-layered square-celled core hollow sandwich cylinders as well as four- and five-layered triangular-core hollow sandwich cylinders are compared in Figs. 15(a–c) for $R_o = 0.12\,\mathrm{m}$ and $L = 2R_o$. More general cases (e.g., $L = 5R_o$ and $L = 10R_o$) have also been studied and the trend is similar to that shown

Please cite this article as: Liu, T., et al., Bi-functional optimization of actively cooled, pressurized hollow sandwich cylinders with prismatic..., J. Mech. Phys. Solids (2007), doi:10.1016/j.jmps.2007.04.007

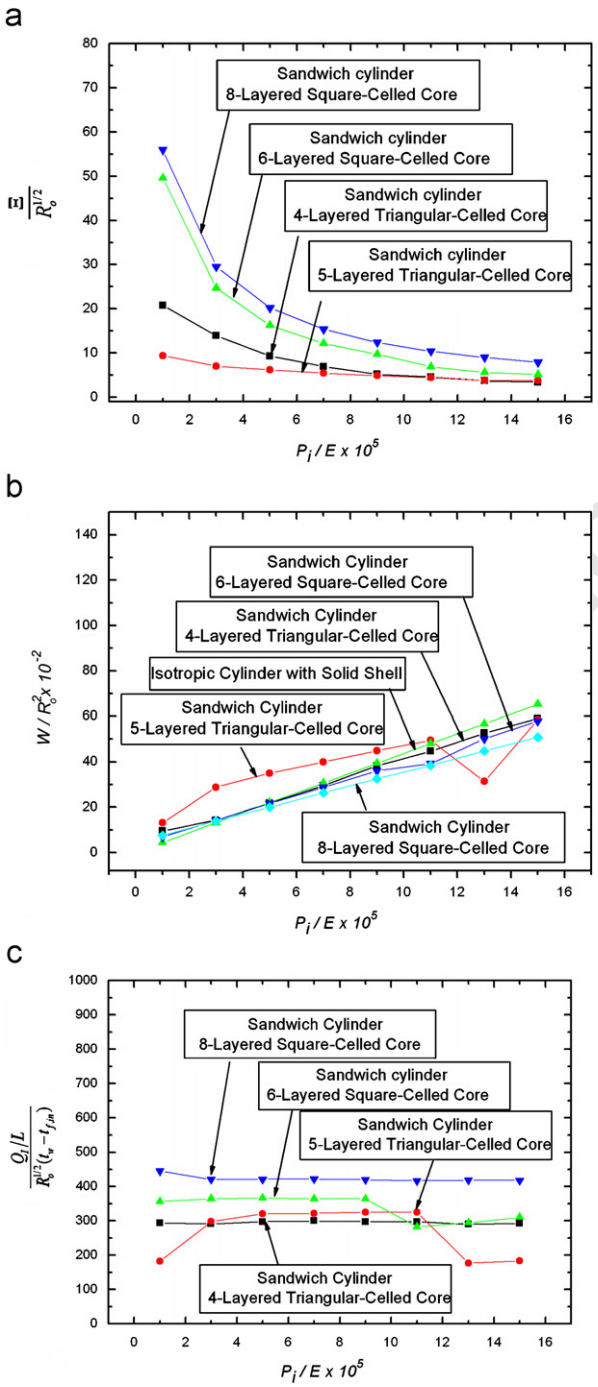

Fig. 15. Comparison of: (a) $\Xi/R_o^{1/2}$; (b) W/R_o^2 and (c) $(Q_I/L)/R_o^{1/2}(t_w - t_{f,in})$, each plotted as a function of dimensionless load parameter, for optimally designed eight- and six-layered sandwich cylinders having square cells and four- and five-layered triangular-core sandwich cylinders, all calculated with $R_o = 0.12\,\mathrm{m}$, $L = 2R_o$, $\kappa = 1$, $k_s = 60.5\,\mathrm{W/mK}$, $\rho_s = 7900\,\mathrm{kg/m^3}$, $\xi \geqslant 0.8$, $\widehat{P} = 0.5\,\mathrm{W}$, $v = 0.3$, $\sigma_Y/E = 0.001$, $T_J/R_o \geqslant 0.001$ $(J = \mathrm{i,c,o})$, $0.9 \geqslant R_i/R_o \geqslant 0.5$ and based on *maximum* $\Xi/R_o^{1/2}$ *design model*; the working coolant is air.

in Fig. 15. These results demonstrate that the bi-functional performance of triangle-celled sandwich cylinders is not as good as that of square-celled ones. When the cylinders are relatively short ($L \leqslant 5R_o$), the value of W/R_o^2 for triangular-celled sandwiches is usually greater than or equal to that of a solid-walled cylinder (Fig. 15b). Furthermore, different from square-celled core sandwiches, the failure mode is the buckling of inclined core members.

7. Concluding remarks

The thermo-mechanical performance of hollow sandwich cylinders with 2D prismatic cores is investigated. The cylinder, pressurized internally and, with its inner surface maintained at a constant temperature, is simultaneously cooled by forced convection. The structural advantage of the sandwich wall construction relative to that of a monolithic-walled cylinder is firstly demonstrated by minimum mass optimization. With the intersection-of-asymptotes method, developing laminar flow and temperature field are subsequently considered in the optimization model for maximum heat dissipation. The optimal geometry corresponding to the maximum heat dissipation is found to be not unique.

A non-dimensional parameter is introduced to couple the structural and thermal objectives in a single bi-objective function. With pumping power fixed and air used as coolant, square-celled core sandwich cylinders outperform those having triangular cells in terms of thermo-mechanical performance. It is further demonstrated that eight-layered sandwich cylinders with square cells have the best overall thermo-mechanical performance. To this end, the core topology needs to be optimized for maximum heat transfer performance, whilst the facesheet thickness (that of the inner facesheet in particular) must be optimized to support the internal pressure at minimum mass. It is beneficial to shorten the length of the cylinder, whilst the outer radius of the cylinder has only a minimal influence.

The analytical method employed for heat transfer under forced convection within this paper is generally based on the assumption that the flow is laminar in the 2D core passages (as mentioned in Section 1). In 3D structures such as truss core sandwiches, the flow in the channels is usually turbulent even at relatively low Reynolds numbers. Hence, in the absence of a suitable analytical heat transfer model for 3D structures, the present model cannot be extended to such cases: a full numerical approach is required which would be extremely time consuming.

8. Uncited reference

Liu et al. (2007).

Acknowledgments

The authors wish to thank the National Basic Research Program of China (2006CB601202), the National Natural Science Foundation of China (10328203, 10572111, 10572119, 10632060), the National 111 Project of China (B06024), the Program for New Century Excellent Talents in University (NCET-04-0958), the Open Foundation of State Key Laboratory of Structural Analysis of Industrial Equipment, and the

Please cite this article as: Liu, T., et al., Bi-functional optimization of actively cooled, pressurized hollow sandwich cylinders with prismatic..., J. Mech. Phys. Solids (2007), doi:10.1016/j.jmps.2007.04.007

Doctorate Foundation of Northwestern Polytechnical University for supporting this work. TJL would also like to thank his former student Matthew Raskie for discussions during the initial stage of this research.

Appendix A

To elucidate why an internally pressurized hollow sandwich cylinder structurally outperforms its equivalent solid-walled cylinder, analytical solutions of the minimum masses for both solid-walled cylinder and single-layered sandwich cylinder with square cells are presented for comparison.

A.1. Minimum mass of a solid-walled cylinder

Using the Lamé equations (Timoshenko and Young, 1956), the maximum stresses within an internally pressurized hollow solid-walled cylinder can be written as:

$$\sigma_{\theta,\max} = P_i \frac{1 + R_i^2/R_o^2}{1 - R_i^2/R_o^2}, \quad \sigma_{R,\max} = -P_i, \tag{78}$$

where σ_R and σ_θ are the radial and circumferential normal stresses, respectively.

Hence, the structural mass of the cylinder per unit length, $W/R_o^2 = \rho_s \pi(1 - R_i^2/R_o^2)$, becomes minimum when

$$\frac{\sigma_{\text{Von},\max}}{E} = \frac{\sqrt{2}}{2}\left\{\left(\frac{\sigma_{\theta,\max}}{E} - \frac{\sigma_{R,\max}}{E}\right)^2 + \left(\frac{\sigma_{R,\max}}{E}\right)^2 + \left(\frac{\sigma_{\theta,\max}}{E}\right)^2\right\}^{1/2} = \frac{\sigma_Y}{E}, \tag{79}$$

where σ_{Von} is the von Mises stress and, for simplicity, the contribution of through-thickness stress σ_Z is ignored. Obviously, for $\sigma_Y/P_i \gg 1$ (as considered in this paper), we have

$$\frac{W_{\min}}{R_o^2} = \frac{2\pi\rho_s P_i}{\sigma_Y}. \tag{80}$$

That is to say, the minimum mass of a structurally optimized solid-walled cylinder varies linearly against P_i.

A.2. Minimum mass of a single-layered sandwich cylinder with square cells

As mentioned in Section 4.2, the failure modes of a structurally optimized sandwich cylinder subjected to internal pressure loading are simultaneous inner facesheet yielding and core member buckling. Hence, from (73), we have

$$\frac{\sigma_{x,1}^c}{E} = \frac{\kappa\pi^2(T_{c1}/R_o)^2}{12(1-v^2)[(T_c - T_o/2 - T_i/2)/R_o]^2}, \tag{81}$$

where $\sigma_{x,1}^c$ is the normal stress in the x direction for vertical core members (Fig. 5d), with the buckling coefficient $\kappa = 1$ for the simply supported case. By (62), we have

$$P_{a,1} = \frac{E\pi^2(T_{c1}/R_o)^3}{24(1-v^2)(p/R_o)[(T_c - T_o/2 - T_i/2)/R_o]^2}, \tag{82}$$

Please cite this article as: Liu, T., et al., Bi-functional optimization of actively cooled, pressurized hollow sandwich cylinders with prismatic..., J. Mech. Phys. Solids (2007), doi:10.1016/j.jmps.2007.04.007

$$P_{b,1} = \frac{E\pi^2 (T_{c1}/R_o)^3 (R_i/R_o)}{24(1-v^2)(p/R_o)[(T_c - T_o/2 - T_i/2)/R_o]^2}. \tag{83}$$

From Eqs. (55) and (56), the maximum stresses in both the inner and outer facesheets can be written as

$$\sigma^i_{\theta,\max} \approx (P_i - P_{a,1}) \frac{(R_i + T_i)^2 + (R_i - T_i)^2}{(R_i + T_i)^2 - (R_i - T_i)^2}, \quad \sigma^i_{R,\max} \approx -(P_i - P_{a,1}), \tag{84}$$

$$\sigma^o_{\theta,\max} = P_{b,1} \frac{(R_o + T_o)^2 + (R_o - T_o)^2}{(R_o + T_o)^2 - (R_o - T_o)^2}, \quad \sigma^o_{R,\max} = -P_{b,1}. \tag{85}$$

Hence, the structural masses per unit length of both facesheets, $W^\lambda/R_o^2 = \rho_s \pi((R_\lambda + T_\lambda)^2 - (R_\lambda - T_\lambda)^2)/R_o^2$, $(\lambda = i, o)$, become minimum when

$$\frac{\sigma^\lambda_{\text{Von},\max}}{E} = \frac{\sqrt{2}}{2} \left\{ \left(\frac{\sigma^\lambda_{\theta,\max}}{E} - \frac{\sigma^\lambda_{R,\max}}{E} \right)^2 + \left(\frac{\sigma^\lambda_{R,\max}}{E} \right)^2 + \left(\frac{\sigma^\lambda_{\theta,\max}}{E} \right)^2 \right\}^{1/2} = \sigma_Y/E. \tag{86}$$

Thence, for the case of $\sigma_Y/P_i \gg 1$, we have

$$W^i_{\min}/R_o^2 = \frac{\pi\rho_s(P_i - P_{a,1})}{R_o^2 \sigma_Y}[(R_i + T_i)^2 + (R_i - T_i)^2], \tag{87}$$

$$W^o_{\min}/R_o^2 = \frac{\pi\rho_s P_{b,1}}{R_o^2 \sigma_Y}[(R_o + T_o)^2 + (R_o - T_o)^2]. \tag{88}$$

Subsequently, the total mass per unit length of a single-layered sandwich cylinder with square cells, which satisfies both Eqs. (81) and (86), can be written as

$$W^*/R_o^2 = \frac{\pi\rho_s(P_i - P_{a,1})}{R_o^2 \sigma_Y}[(R_i + T_i)^2 + (R_i - T_i)^2] + \frac{\pi\rho_s P_{b,1}}{R_o^2 \sigma_Y}[(R_o + T_o)^2 + (R_o - T_o)^2] + \frac{\pi\rho_s R_i}{p} \frac{(T_c - T_o/2 - T_i/2)T_{c1}}{R_o^2}. \tag{89}$$

For $T_j/R_o \geqslant 0.001$ $(j = i, c)$, $T_o/R_o = 0.001$ (lower bound), $v = 0.3$, $T_c/R_o = 0.5$ and $p/R_o = 0.157$ (upper bound), by $\partial(W^*/R_o^2)/\partial T_c = 0$ and $\partial(W^*/R_o^2)/\partial T_i = 0$, we have

$$W^*_{\min}/R_o^2 \approx \frac{0.66\pi\rho_s P_i}{\sigma_Y} < W_{\min}/R_o^2 = \frac{2\pi\rho_s P_i}{\sigma_Y}. \tag{90}$$

As shown above, the minimum mass of a single-layered sandwich cylinder having square cells varies linearly against P_i and is about 2 times lighter than that of an optimized solid-walled cylinder.

References

Bejan, A., Sciubba, E., 1992. The optimal spacing of parallel plates cooled by forced convection. Int. J. Heat Mass Transfer 35, 3259–3264.

Gu, S., Lu, T.J., Evans, A.G., 2001. On the design of two-dimensional cellular metals for combined heat dissipation and structural load capacity. Int. J. Heat Mass Transfer 44, 2163–2175.

Hutchinson, J.W., He, M.Y., 2000. Buckling of cylindrical sandwich shells with metal foam cores. Int. J. Solids Struct. 37, 6777–6794.

Please cite this article as: Liu, T., et al., Bi-functional optimization of actively cooled, pressurized hollow sandwich cylinders with prismatic..., J. Mech. Phys. Solids (2007), doi:10.1016/j.jmps.2007.04.007

Hutchinson, R.G., Wicks, N., Evans, A.G., Fleck, N.A., Hutchinson, J.W., 2003. Kagome plate structures for actuation. Int. J. Solids Struct. 40, 6969–6980.

Kim, T., Zhao, C.Y., Lu, T.J., Hodson, H.P., 2004. Convective heat dissipation with lattice-frame materials. Mech. Mat. 36, 767–780.

Lekhnitskiæi, S.G., 1981. Theory of Elasticity of an Anisotropic Body. Mir Publishers, Moscow.

Liu, T., Deng, Z.C., Lu, T.J., 2006. Design optimization of truss-cored sandwiches with homogenization. Int. J. Solids Struct. 43, 7891–7918.

Liu, T., Deng, Z.C., Lu, T.J., 2007. Minimum weights of pressurized hollow sandwich cylinders with ultralight cellular cores. Int. J. Solids Struct. 44, 3231–3266.

Lu, T.J., 1998. Heat transfer efficiency of metal honeycombs. Int. J. Heat Mass Transfer 42, 2031–2040.

Lu, T.J., Chen, F., He, D.P., 2000. Sound absorption of cellular metals with semiopen cells. J. Acoust. Soc. Am. 108, 1697–1709.

Lu, T.J., Valdevit, L., Evans, A.G., 2005. Active cooling by metallic sandwich structures with periodic cores. Progr. Mater. Sci. 50, 789–815.

Muzychka, Y.S., Yovanovich, M.M., 2004. Laminar forced convection heat transfer in the combined entry region of non-circular ducts. J. Heat Transfer—Trans. ASME 126, 54–61.

Muzychka, Y.S., Yovanovich, M.M., 2002. Laminar flow friction and heat transfer in non-circular ducts and channels: Part I—hydrodynamic problem, in Compact Heat Exchangers: A Festschrift on the 60th Birthday of Ramesh K. Shah. Grenoble: France. pp. 123–130.

Raskie, M.J., 2006. Concentric Tube Heat Exchangers as Combustion Chambers. M.Phil. Thesis, Cambridge University Engineering Department.

Ruzzene, M., 2004. Vibration and sound radiation of sandwich beams with honeycomb truss core. J. Sound Vib. 277, 741–763.

Shah, R.K., London, A.L., 1978. Laminar Flow Forced Convection in Ducts: a Source Book for Compact Heat Exchanger Analytical Data. Academic Press, New York.

Tian, J., Kim, T., Lu, T.J., Hodson, H.P., Queheillalt, D.T., Sypeck, D.J., Wadley, H.N.G., 2004. The effects of topology upon fluid-flow and heat-transfer within cellular copper structures. Int. J. Heat Mass Transfer 47, 3171–3186.

Timoshenko, S., Young, D.H., 1956. Engineering Mechanics. McGraw-Hill, New York; London.

Valdevit, L., Hutchinson, J.W., Evans, A.G., 2004. Structurally optimized sandwich panels with prismatic cores. Int. J. Solids Struct. 41, 5105–5124.

Valdevit, L., Pantano, A., Stone, H.A., Evans, A.G., 2006a. Optimal active cooling performance of metallic sandwich panels with prismatic cores. Int. J. Heat Mass Transfer 49, 3819–3830.

Valdevit, L., Wei, Z., Mercer, C., Zok, F.W., Evans, A.G., 2006b. Structural performance of near-optimal sandwich panels with corrugated cores. Int. J. Solids Struct. 43, 4888–4905.

Wen, T., Xu, F., Lu, T.J., 2007. The Structural Optimization of Two-Dimensional Cellular Metals Cooled by Forced Convection. Int. J. Heat Mass Transfer 50, 2590–2604.

Wicks, N., Hutchinson, J.W., 2001. Optimal truss plates. Int. J. Solids Struct. 38, 5165–5183.

Wicks, N., Hutchinson, J.W., 2004. Sandwich plates actuated by a Kagome planar truss. J. Appl. Mech.—Trans. ASME 71, 652–662.

Xue, Z.Y., Hutchinson, J.W., 2003. Preliminary assessment of sandwich subject to blast loads. Int. J. Mech. Sci. 45, 687–705.

Xue, Z.Y., Hutchinson, J.W., 2006. Crush dynamics of square honeycomb sandwich cores. Int. J. Numer. Methods Eng. 65, 2221–2245.

Yilmaz, A., Buyukalaca, O., Yilmaz, T., 2000. Optimum shape and dimensions of ducts for convective heat transfer in laminar flow at constant wall temperature. Int. J. Heat Mass Transfer 43, 767–775.

Please cite this article as: Liu, T., et al., Bi-functional optimization of actively cooled, pressurized hollow sandwich cylinders with prismatic..., J. Mech. Phys. Solids (2007), doi:10.1016/j.jmps.2007.04.007